

Micro Gas Turbine thermal emulator set-up in a real-time environment

Author

Ander Retamosa

Reviewer 1

Prof. Dr. Veit Hagenmeyer

Reviewer 2

Prof. Dr. Mathias Noe

Tutor

Eng. Dustin Kottonau

Advisor

Dr. Giovanni de Carne

Micro Gas Turbine thermal emulator set-up in a real-time environment

Abstract

Energy field has become a key sector in the world. Thermal systems have become increasingly more important in the energy field and due to this this project aims to make a step forward regarding the thermal system technology. The objective of this work is selecting a thermal device, a micro gas turbine in this case, and try to emulate its thermal behaviour. For doing so, a thermal emulator has been modelled and set-up in a real-time environment. The model made includes the hole hydraulic analysis of the thermal emulator. This model has been achieved by two different paths. Using a mathematical theoretical model and a physical Matlab Simscape model. These models have been, afterwards, compared with the set-up results. Results show that flow is going to be used to controlling the transient state of the thermal power of the pump, while electric power is going to be used to reach the desired set-point. Overall, results show that it is possible to emulate the behaviour of the micro gas turbine and that the objective of this work has been fulfilled.

Keywords: Thermal Emulator, Micro Gas Turbine, Real-time Simulation, Thermal Power, Rate of Change, Steady state, Transient State

Contents

1	Introduction	2
2	Application and impact	5
3	Thermal Emulator	8
3.1	Theoretical Analysis of the components	9
3.1.1	Principal elements of the set-up	9
3.1.1.1	Pump	9
3.1.1.2	Heat Exchanger	13
3.1.1.3	Electric Heater	16
3.1.2	Secondary elements of the set-up	17
3.2	Creation of Models	18
3.2.1	Fluid mechanics pressure drop theory	18
3.2.2	Mathematical based model	23
3.2.2.1	OP calculation	25
3.2.2.2	Maple pressure drop results	29
3.2.3	Simulation based model	31
3.2.3.1	Model parameters	32
3.2.3.2	Matlab Simscape model results	36
3.2.4	Model and Theoretical Results comparison	39
3.3	Laboratory Set-up	41
3.3.1	Grundfos pump CRE 3-4 A-A-A-E-HQQE	42
3.3.2	Heat Exchanger Güntner, FLAT COMPACT GFHC	45
3.3.3	Electric Heaters Walser	46
3.3.4	Electric Amplifiers	47
3.3.5	Electric Valve	48
3.3.6	Pressure Diaphragm Vessel	49
3.3.7	Pressure, temperature and flow transmitters	49
3.4	Experimental Results Analysis	52
3.4.1	Measurement and Uncertainty	52
3.4.2	Model Validation	53
3.4.3	Maximum Rate of Change	58
3.4.4	Limits of Applicability	63
4	Real modelling on virtual household	64
4.1	RTDS real time simulator and MGT behavior target	64
4.2	Electric variable power PI controller to control thermal power	67
4.3	MGT and thermal emulator comparison and discussion	68

5	Conclusions	70
A	Appendix	72
	Bibliography	77

List of Figures

1.1	Gross electricity production in Germany amounted to 565 terrawatt hours in 2020 (preliminary data). The chart shows the distribution by energy source in percent, status: April 2021[23]	2
1.2	Household schema including both the MGT and the thermal emulator	4
2.1	A simplified diagram of a gas-fired micro-gas turbine CHP system [1]	6
3.1	Simplified schema of the laboratory set-up	8
3.2	Centrifugal vertical pump schema and working principle [15]	10
3.3	Example of an operation point of a pump	12
3.4	Classification of HE [16]	13
3.5	Moody Diagram	21
3.6	Mathematical simplified model	23
3.7	Grundfos pump characteristic Curves [14]	25
3.8	Comparison between the real and linearized curve with manufacturer's curve	28
3.9	OP	28
3.10	Matlab Simscape full model	31
3.11	Matlab Simscape Grundfos pump model	34
3.12	Matlab Simscape pipe and HE model	36
3.13	Correlation pump rotation speed $\dot{\omega}$ [rpm] and Flow \dot{Q} [l/min] theoretical and approximation	38
3.14	Maple vs Simscape mathematical and model comparison of the results	40
3.15	Laboratory set-up overview of all the elements	41
3.16	Grundfos CRE 3-4 A-A-A-E-HQQE PUMP [14]	42
3.17	Heat exchanger laboratory set-up	45
3.18	Electric Heaters laboratory set-up	46
3.19	Spitzenberger amplifier laboratory set-up	47
3.20	IMI Hydronic TA-Slider 160 electric valve[7]	48
3.21	Reflex N25 pressure diaphragm vessel [18]	49
3.22	IFM PT0505 pressure transmitter [11]	50
3.23	IFM TA3317 temperature transmitter [12]	51
3.24	IFM SM6000 flow transmitter [10]	51
3.25	Pump controlled HE pressure drop during time for different flows, due to a change in the pump input electric signal	54
3.26	Valve controlled HE pressure drop during time for different flows, due to a change in the valve input signal with pump signal constant	54
3.27	Valve controlled HE pressure drop for low pump rotating speed	55
3.28	Correlation between flow and HE pressure drop for pump and valve controlled cases	55
3.29	Model and experimental results comparison regarding the flow and HE pressure drop	56
3.30	Pump controlled flow rate of change	58
3.31	Valve controlled flow rate of change	58

3.32	Detail of rate of change pump and valve controlled	59
3.33	Flow variable and electric power constant thermal power rate of change analysis A	60
3.34	Flow variable and electric power constant thermal power rate of change analysis B	60
3.35	Flow variable and electric power constant thermal power rate of change analysis detail A for 9V pump signal	60
3.36	Flow variable and electric power constant thermal power rate of change analysis detail B for 2V pump signal	60
3.37	Electric power variable and flow constant thermal power rate of change analysis A	61
3.38	Electric power variable and flow constant thermal power rate of change analysis B	61
3.39	Detail of electric power variable and flow constant thermal power rate of change analysis to evaluate thermal power rate of change	62
3.40	Amplifier security switch off above 90°C	63
4.1	NovaCor RTDS custom-built board unit [26]	64
4.2	NovaCor RTDS connection to device under test[26]	65
4.3	GTAI analogue card[26]	66
4.4	MGT real device behavior and target	66
4.5	PI controller for thermal power using a variable electric power	67
4.6	Comparison between Micro Gas Turbine and Thermal Emulator thermal power output and transient behaviour	68
4.7	Detail of the comparison between Micro Gas Turbine and Thermal Emulator thermal power output to analyze the transient behaviour	69
A.1	Matlab Simscape full model	73
A.2	Sensor electrical connection input GTAIRTDS card	74
A.3	Principal elements electrical connection output GTAIRTDS card	75
A.4	Full hydraulic drawing including all the necessary elements for the construction of the set-up	76

List of Tables

2.1	Comparison between the real MGT and the thermal emulator	6
3.1	Pressure drop problem variable description and units	24
3.2	Pressure drop problem data	24
3.3	Variable and constants characteristic curve units and values	26
3.4	conversion factors	26
3.5	OP	29
3.6	OP error	29
3.7	Pressure drop results obtained on Maple]	29
3.8	Head $H[m]$ table $[\dot{Q},\dot{\omega}]$ parameterization	32
3.9	Brake power $W_b[kW]$ table $[\dot{Q},\dot{\omega}]$ parameterization	33
3.10	Centrifugal pump rest of the parameters	33
3.11	HE parameterization	34
3.12	Pipe system parameterization	35
3.13	Matlab Simscape pressure drop calculations according to different rotational speeds	37
3.14	Comparison OP Simscape model and manufacturer curve	37
3.15	Pipe system pressure drop comparison Mathematical and model and error	39
3.16	HE pressure drop comparison .Mathematical and model and error	39
3.17	Grundfos pump manufacturer technical data [14]	43
3.18	User information about Grundfos pump operation points	44
3.19	Güntner HE manufacturer technical data [9]	45
3.20	Güntner HE tube data [9]	46
3.21	Walser electric heater data [3]	46
3.22	Spitzenberger Spies amplifier data [22]	47
3.23	TA Slider 160 IMI Hydronic electric valve data [7]	48
3.24	Reflex N25 pressure diaphragm vessel data [18]	49
3.25	IFM PT050 pressure transmitter data [11]	50
3.26	IFM TA3317 temperature transmitter data[12]	50
3.27	IFM 6000 flow transmitter data [10]	51
3.28	Overview of sensor lower and upper measuring range and uncertainty [11][10][12]	52
3.29	Maximum and minimum values of thermal power of the thermal emulator according to un- certainty range	53
3.30	Comparison model and experimental results and error	56
3.31	Temperatures in °C for different combinations of flow and electric power supply	62

Chapter 1

Introduction

Energy transition in the electricity sector is a global issue that concerns almost all governments all over the world. In the particular case of Germany, the share of renewable energies in gross electricity consumption has risen to 45 percent in 2020. This renewable energy share is largely constituted by wind energy, biomass and photovoltaic plants, followed by hydropower and geothermal energy.

The biggest problem the world faces so far is the difficulty to store big amounts of electricity, at least in a notorious way. That is the reason why we need the support of the conventional power plants so as to cover the electricity demand when there is no enough wind or sun, for instance. These conventional plants must respond flexibly to fluctuations, which means that they must be able to operate cost- and resource-efficiently in partial- and minimum load-operation.

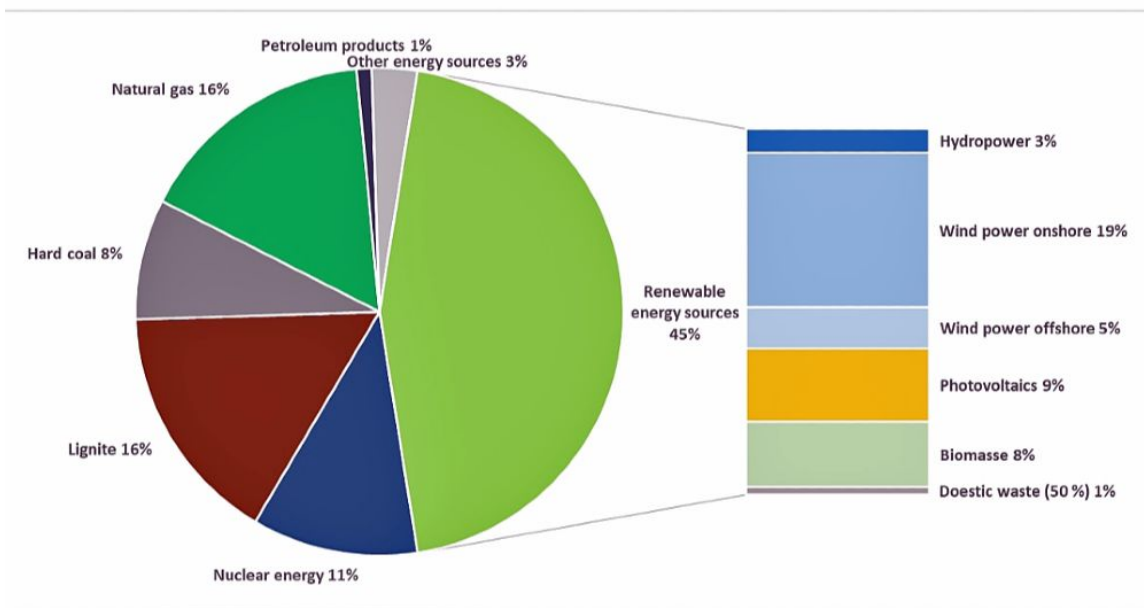


Figure 1.1: Gross electricity production in Germany amounted to 565 terrawatt hours in 2020 (preliminary data). The chart shows the distribution by energy source in percent, status: April 2021[23]

Considering that the mix between the renewable energy and the conventional plant is still

going to be part of us, both sources must be optimally interlinked in order to successfully transform the energy system. This transformation should be done in a climate-friendly and sustainable way. For this reason, research into future-proof power generation technologies is an important mainstay in this context.

German government plans to transform the country's energy supply by 2045. The main goal is to increase the energy efficiency and to achieve climate neutrality by then. In this context play a key role the future-proof power generation technology[23].

With the energy transition, Germany is bidding farewell to nuclear and fossil fuels for heat and power generation. The first of option instead of using these energy generation modes, is a combination between wind and sun mostly. For this purpose, on July 2020, the Federal German Government passed the Coal Phase-out Act. This act established further binding steps in the transformation of the energy system, being the central target: No coal is to be used for power generation by 2038 at the latest.

These binding steps have led a change in research priorities regarding thermal power plants. While they were in continuous operation just a few years ago, in times of the energy transition, they are becoming an on-demand support tool when photovoltaic and wind energy are not sufficient to cover the energy supply demanded.

Although the renewable energies are pushing strongly, thermal power plants continue to play a decisive role in the restructuring of the energy system. There is a trend now that supports alternative fuels and fuel mixtures such as biomass or waste instead of coal in power plant operations.

As far as thermal renewable power plants are concerned, research is being done in solar thermal and geothermal power plants fields. In Germany they only exist as demonstration installations because of the low direct solar irradiation. Due to this, research is being done in order to export the know how to other parts of the world, such as Spain or Morocco, where the solar irradiation is much higher.

Additionally, there is as well research ongoing regarding gas turbines field. Gas and steam turbines must be optimized and further developed for combined operation in gas and steam power plants or in combined heat and power plants. It is said that the gas turbines will be a building block of the energy transition[24]. According to this last cite, our goal was to make an impact on gas turbines line, indeed, in the micro gas turbines. Making use of a MGT, the idea is to obtain heat using a combination of elements in parallel with the MGT for house heating. The set-up is connected to a thermal load that will be the responsible for heating the household.

The problem comes in an ordinary situation, as the house has a new owner and the MGT installed in the house has not enough power to feed the requirements of the new house owner. Some solutions are possible to resolve this situation. At a first time, the idea of installing a new MGT in parallel with the already installed one attracted the new owner. Nevertheless, it would bring a relative high cost. An alternative to installing a new MGT is a thermal emulator. The objective of this new set-up is not only reducing the cost of the installation, but also to be more flexible and reliable. In order to have a general idea regarding this new

set-up, a schema of the new building is attached.

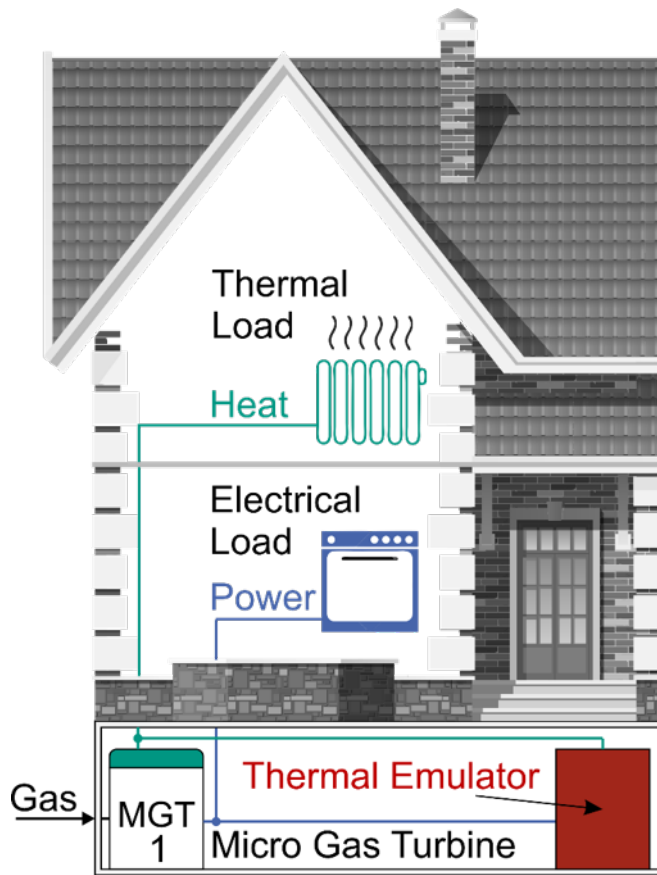


Figure 1.2: Household schema including both the MGT and the thermal emulator

The main objective of this installation is obtaining the same response as the MGT in a more flexible, economic and reliable way. For this reason, the guideline of this thesis is making an exhaust analysis of this thermal emulator, studying it's viability, comparing to the MGT and finally studying the future application of this revolutionary set-up. The idea, in the future, is not only to be behave as a MGT, but to emulate other thermal set-ups.

Chapter 2

Application and impact

The thermal emulator will emulate the behavior of a MGT. The idea in the future is to make further research on the thermal emulator so as to emulate not only this type of technology, but other type of technologies which have to do with heat transfer. Some examples of these other technologies could be a fuel-cell or a combined cycle.

In our case, as we are emulating the MGT behavior, we are going to focus on developing and understanding the basis of a MGT. Micro-gas turbines are small combustion gas turbines with power output ranging from 30 kW to over 200 kW. The power reduction of this machines, comparing to conventional gas turbines, has a negative impact on the power output and efficiency, affecting heat and combustion processes. In order to reduce this negative impact these micro-gas turbines operate at a very high rotational speed (up to 100 000 rpm) and make use of electronic power inverters to generate a.c. voltage at grid frequency. At the same time, a heat recuperator is also introduced for the exhaust hot gases so as to pre-heat compressed combustion air. This leads to a significant reduction of the fuel consumption and an improvement of the global electrical efficiency, up to 30. Although this electrical efficiency seems not so great, due to the recuperator, the thermal efficiency could reach 80.

A typical micro-gas turbine is based on the Brayton cycle and it is built with the following components:

- Combustor: This is the chamber where the combustion chemical reaction happens concerning fuel and air.
- Turbine: The turbine makes advantage of the gases to make the axis rotate and transmit this rotational movement to the electric generator axis.
- Generator: This generator converts the mechanical rotational energy coming from the turbine into electric energy that will be introduced into the grid.
- Compressor: The compressor will compress the mixture fuel-air to optimal condition for the combustion reaction inside the combustor.
- Recuperator: The recuperator is a key factor in this cycle because it takes advantage of the exhaust hot gases that come from the combustion (at 500-600°C) so as to pre-heat the compressed combustion air saving fuel [20].

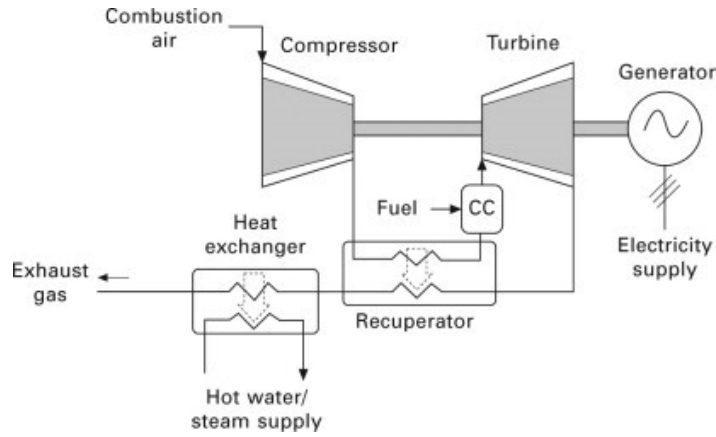


Figure 2.1: A simplified diagram of a gas-fired micro-gas turbine CHP system [1]

MGTs offer the advantages of compact size requiring smaller area to operate; low weight per unit power compared to bigger GT; fewer moving parts so lower maintenance cost are assumed; multi fuel capability and ease of emission control.

The general idea is to emulate this behavior using a thermal emulator that gives the exact output. This idea will lead to emulate not only micro-gas turbines, but other thermal output power devices in the future. The main goal is to gain flexibility having a set-up that can emulate diverse cycles without having the necessity to change the original set-up. Furthermore, this leads into a substantial economical save as the components used are much cheaper than a MGT in this case.

In order to illustrate and clarify a comparison between MGT and a thermal emulator, the following table is shown.

Real vs Emulator comparison		
Characteristics	MGT	Thermal emulator
Cost	High	Low
Accuracy	=	=
Behaviour	better	worse
Flexibility	-	++
Environmental impact	+	-

Table 2.1: Comparison between the real MGT and the thermal emulator

I have decided to use these 5 parameters to compare both construction: cost, accuracy, flexibility and environmental impact.

- Cost: It is the key factor in every project and this is why it on the top of this list. This will mark the viability of the project and the main reason of utilizing a thermal

emulator instead of a MGT. The main difference will not only be into the initial cost, but into the maintenance and operation costs as well. The MGT consists of several moving parts, a combustion chamber and the necessity of fuel. These 3 parameters increase notoriously the overall costs of the installation. The thermal emulator consists basically of a pump and a heat exchanger, being the only moving part the fan. This reduces considerably the costs of maintenance. The lack of fuel is also an economical indicator as we should not worry about the fluctuation of the gas market. However, the use of electric amplifiers will be a relatively important source of cost regarding the hole maintenance costs.

- Accuracy: Accuracy refers to the steady state final value obtained, in this case, we are going to focus on the thermal power. The idea is the steady state to be as accurate as possible, therefore, we could conclude that accuracy should be equal for both devices.
- Behavior: Obviously as it is an emulator, it would be impossible to overhead the accuracy of the real device. This will be key part of the process as it is a must on the research of this topic. Transient behavior of the MGT is not going to be modelled through this work. The objective is to obtain the steady state of the proposed MGT set-point. The transient behavior should be a task for a further optimisation of this device that now is out of the scope of the work.
- Flexibility: Flexibility is one of the key reasons why we implement a thermal emulator. Having the capacity to emulate not only a MGT, but another thermal device as well give us the opportunity to implement this set-up in different systems with no further inversion. This makes this thermal emulator incredibly attractive and competitive comparing to a large number of thermal devices, such as a MGT.
- Environmental impact: This is another key factor due to the world´s current situation. We see a big difference regarding the CO₂ emissions basically due to the combustion process that happens in the inside the combustor to obtain heat. The impact of the thermal emulator is incredibly reduced due to the lack of a combustion reaction. It is true that the electrical heaters have the need of electric power and therefore the environmental impact should be analyzed regarding the source of the electric power.

It is true that this project is in an easy stage and it needs further investigation to optimize cost-functioning factors. At this stage it may be not possible to use an emulator to emulate a full version of MGT, but it could be used in parallel with another MGT in order to avoid the use of a second micro-gas turbine. This will be the idea of this project, utilizing the thermal emulator to use it in parallel with a MGT and analyze how they behave together. For future uses, the idea is to use this thermal emulator without the need of another real device. If this idea works trust-worthily in the future, it could be a great competitor of other thermal devices due to the advantages above mentioned.

Chapter 3

Thermal Emulator

In this chapter I am going to describe the set-up used for the experimental analysis of the thermal emulator. The content of this chapter will include a holistic theoretical description of each of the components that take part in the emulator as well as a theoretical explanation of the functioning of each of them.

To begin with, we can see the simplified schema of the thermal emulator set-up. A more detailed schema is available within the appendix section, but for this initial explanation, this simplified image will be much more understandable.

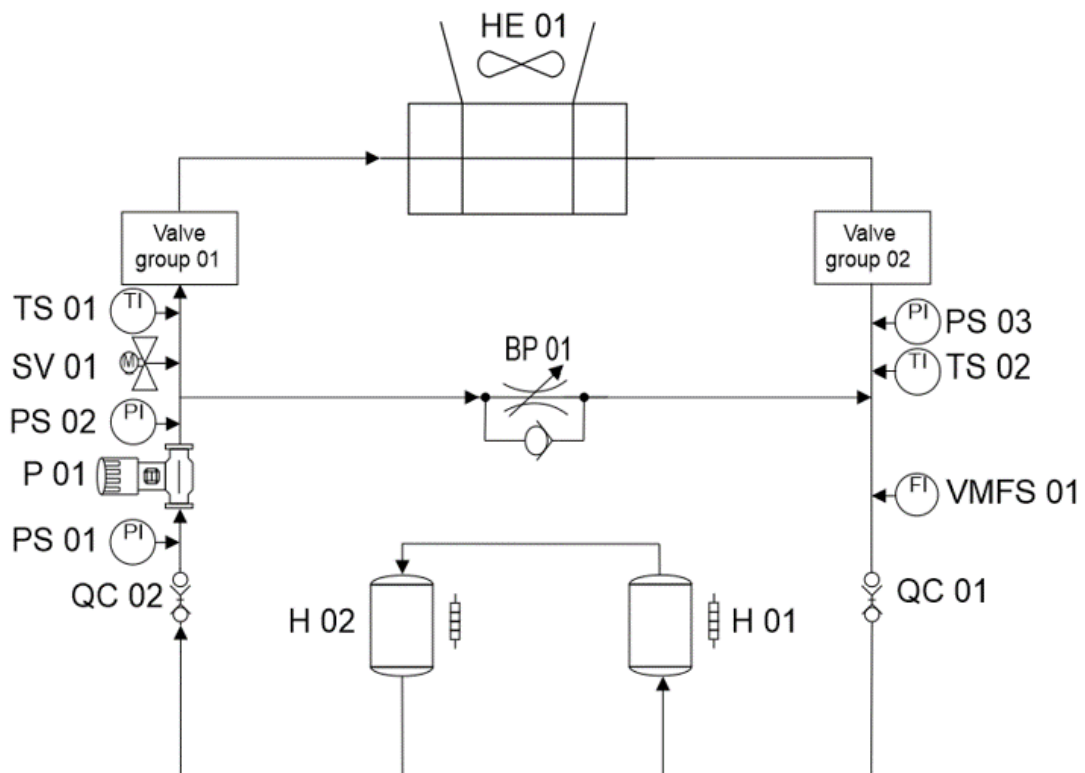


Figure 3.1: Simplified schema of the laboratory set-up

This set-up consists of several parts which I am going to divide into principal and secondary parts. The principal parts consist of a pump, a heat exchanger and two electric heaters. These are the elements that are going mainly to emulate the behavior of the MGT. Additionally, some other elements are crucial for the correct functioning of the emulator. These following elements, complete the thermal emulator set-up: electric valve, mechanical ball-valves, accumulator, amplifiers, by-pass, sensors and quick connectors.

A more exhaust description of the principal elements will be done throughout the following lines and a more overall description of the secondary elements will be done. Generally, a generic structure of the description of the elements will be done to facilitate the comprehension of the reader. The structure will include: general definition and functioning principles, types and components and curves (if it applies).

3.1 Theoretical Analysis of the components

A deeper description of the principal elements will be done throughout the following lines and a more overall description of the secondary elements will be done.

3.1.1 Principal elements of the set-up

Among different elements, we are going to distinguish pump, HE and heaters and explain them in a more detailed way.

3.1.1.1 Pump

A hydraulic pump known as the heart of a hydraulic system is a mechanical source of power that converts mechanical power into hydraulic energy (hydrostatic energy i.e. flow, pressure). It generates flow with enough power to overcome pressure induced by the load at the pump outlet. While mechanical rotational power is the product of torque and speed, hydraulic power is pressure times flow [25].

Among all the machines, the most important ones are the electric-engine and the hydraulic pump. Although the number of users of pumps is incredibly large, the number of pump manufacturers is considerably reduced.

The working principle of these type of hydraulic machines is the same for all the other pumps. Due to external mechanical action powered by an electric supply, the pump creates a partial vacuum at the inlet. This causes the atmospheric pressure to force the fluid into the inlet of the pump due to the vacuum effect. The pump then pushes the fluid into the hydraulic by making use of the rotational system that transmits energy to the fluid [25].

Types and components

There are several ways to classify the hydraulic pumps, but the most general classification names two big groups: Hydrostatic pumps and hydrodynamic pumps. The first group is mainly used for oleo-hydraulic applications and this is out of the scope of this document,

therefore they are going to be only mentioned. Hydrodynamic pumps are the type of pumps that are generally used in the industrial world. This type of pumps could also be divided into two types: Centrifugal and Axial pumps [8].

The type which is most used in the industry field is the centrifugal type. The main difference between these two types is the outlet flow direction. Whereas in the centrifugal type the outlet flow leaves the pump perpendicularly to the intake axis, in the axial type does it parallel to the axis.

Due to the importance of the centrifugal pump, this is the one which is going to be explained on detail from this point on. The centrifugal pump could be defined according to the following lines:

A centrifugal pump is a mechanical device which transfers mechanical rotational energy to the fluid by using it's driven rotors called impellers. Fluid enters the rapidly rotating impeller along its axis (parallel to the intake) and it drives the pressured fluid out by centrifugal force along its variable radius circumference through the impeller's vane tips. The action of the impeller increases fluid's velocity and pressure adding energy to the inlet fluid. After increasing the fluid pressure, the impeller directs it towards the pump outlet perpendicularly to the impeller axis. The pump casing is specially designed to constrict the fluid from the pump inlet by a special device that avoids the top part water fall into the intake, direct it into the impeller and then slow and control the fluid before discharge. In order to clarify this function of the centrifugal pump, a small graphic is hear shown [8].

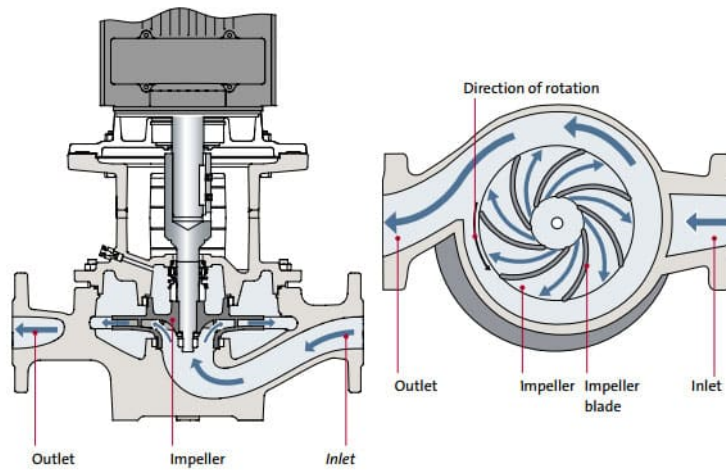


Figure 3.2: Centrifugal vertical pump schema and working principle [15]

This pump is the type of pump is going to be used in the thermal emulator set-up. The hydraulic power of the pump is explained across the following equation.

$$P_H = \rho g H Q \quad (3.1)$$

In this equation, the hydraulic power is expressed by the density of the working fluid ρ , gravity constant g , pump head expressed in meters of column of fluid H and finally the volumetric flow Q .

This is good introduction to what the thermal emulator set-up will look like. According to this image, the following components of the centrifugal pump are described:

- Volute casing: Part that protects all the internal mechanisms that allow the pump to operate. They are made of various materials depending on their purpose, such as cast iron if they will be used to pump drinking water, or stainless steel or bronze if they are intended to pump a liquid that is very corrosive.
- Inlet(suction) and outlet(discharge): The inlet pipe is known as the suction pipe and the outlet pipe is known as the delivery pipe. They are the physical connection with the piping system.
- Impeller: Device used to drive the water contained in the casing. They are made up of a series of blades of various shapes that rotate inside a circular casing. The impeller is attached to the shaft and is the moving part of the pump.
- Volute Chamber: The volute chamber and the impeller are enclosed in the pump casing. The diffuser is made up as a variable circumference section that allows the speed of the water will decrease when the section increase. This helps to transform the kinetic energy into pressure energy, improving the pump's efficiency.
- Shaft: Element that supports the impeller so that it rotates on it with the force of the motor. Depending on the position of the shaft, we distinguish horizontal shaft pumps and vertical shaft pumps.
- Drive shaft: Parts that properly support the impeller shaft. It has mainly mechanical function and it has nothing to do with the fluid.
- Motor: fundamental component of the centrifugal pump that moves the shaft and in turn the impeller to move the water. It is located in the upper part of the pump.

Pump curve

A pump is defined by its characteristic curve. This curve relates the pump head, or the pressure added to the system, to the flow rate. This curve is indicative of the ability of the pump to add energy as pressure at different flow rates. This curve will be crucial for the modelling part as we need to compare the characteristic curve of the pump and the system characteristic curve in terms of head(pressure) and flow. The characteristic point of the pump will be always delivered by the manufacturer. This crossing point between both curves will give the information of the most effective operation point of the system.

The system operating point is based on the point at which the pump curve crosses the system curve representing the static lift and head losses due to friction and minor losses. When both curves meet on a single point, the operating point can easily be found. This is shown in the figure below.

The manufacturer gives information regarding the pump characteristic curve for different speed rotation. This means that we have information for different combinations head-flow

and that we are going to use the best fit for our specific system. These curves are a key parameter for pump modelling and are going to be mentioned again throughout this document. This a little introduction to the OP point of the pump to have a general idea what exactly it is this concept. Actually, this concepts will be in detail explain during the theoretical explanation of the OP, where every step is explained [4].

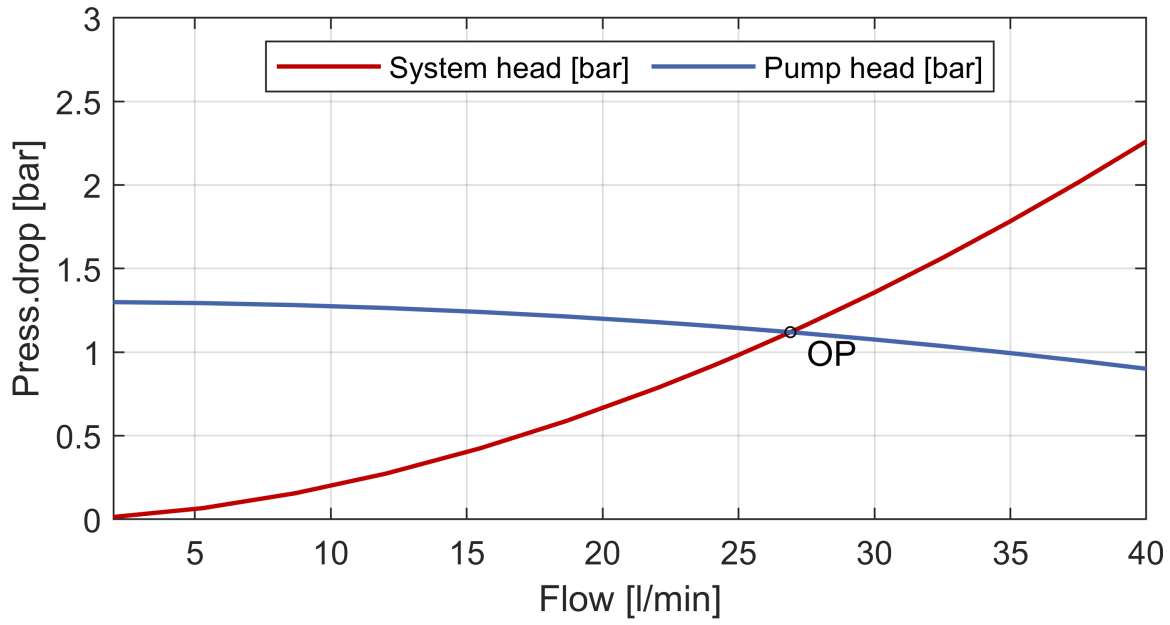


Figure 3.3: Example of an operation point of a pump

3.1.1.2 Heat Exchanger

A heat exchanger is a device which has the principal objective of transferring thermal energy (enthalpy) between two or more fluids, a solid surface and a fluid or between solid particles. Heat exchangers take advantage of the heat of a fluid/solid and transfer it to another without the interaction of an external heat or work interaction.

This heat between the two or more mediums happens normally indirectly, using a wall that separates both mediums and which maintains both mediums isolated. There are some cases that the mediums are actually in touch, but it is not a common situation. Generally, the heat transfer happens in an indirect way by conduction through the separating wall. Inside the heat exchanger could also be some devices that help the heat exchange to happen, such as mechanical devices (fan) to optimize and accelerate the heat flux [16].

Types and components

There are several criteria to classify heat exchangers. The scope of this document is giving a general overview of this elements; therefore, a holistic insight of the classification will be explained in the following lines.

Heat exchangers could be classified according to the following characteristics: transfer process (direct-indirect contact), number of fluids, surface compactness(gas-liquid-solid), heat exchanger construction features, flow arrangements and heat transfer mechanisms. The most important classification in order to select and detect the type of heat exchanger, are the construction feature and flow arrangement classification, whereas the others are more simple ones. To better understand these two classifications, the following schema is helpful.

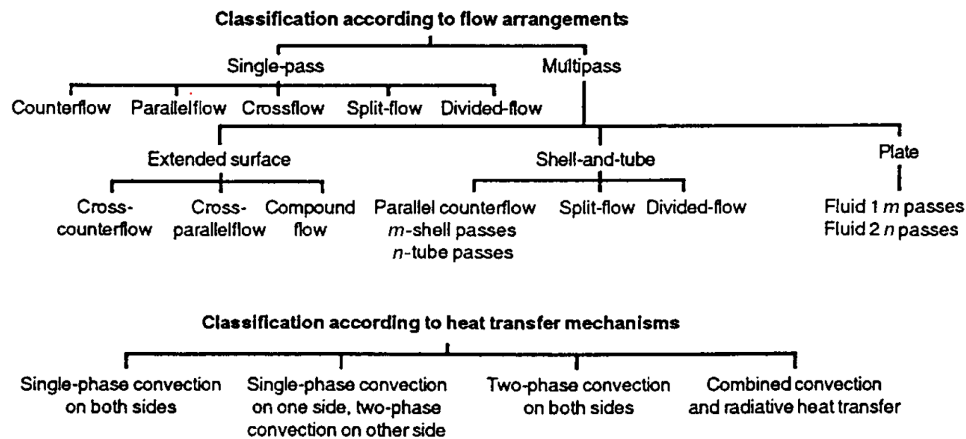


Figure 3.4: Classification of HE [16]

Regarding the construction classification, for set-up similar to the thermal emulator the most used type is the tubular type as at least one of the fluids flows thorough the pipes. This is the most commonly used type of heat exchanger regarding the construction classification. Inside it, several types of heat exchanger could be found and all of them are in the industry

used. The criteria to select one or the other, deals with the available space, cost and second fluid to perform the heat exchange. As an example, if the fluid to refrigerate the circuit fluid was air, having a shell and tube construction would be advisable, with a cross-flow to main fluid direction for example. Introducing a mechanical element, such as a fan, to have forced convection will increase the efficiency of the heat exchanger. The flow arrangement classification will be the next step after having chosen the construction. This selection will depend not only on the construction, but on the type of fluid as well.

Thermal and hydraulic design of a HE

Heat exchanger thermal/hydraulic design procedures involve exchanger rating (quantitative heat transfer and pressure drop evaluation). Only two important relationships constitute the entire thermal design procedure and /or exchanger sizing.

1. Enthalpy rate equations

$$q = q_j = \dot{m}_j \Delta h_j \quad (3.2)$$

one of each of the each of the fluids, being $j=1,2$ designed for each fluid.

2. Heat transfer rate equation

$$q = UA\Delta T_m \quad (3.3)$$

Equation 3.2 is a well-known relationship from thermodynamics. It relates the heat transfer rate q with the enthalpy rate change Δh_j for an open non-adiabatic system with a single flow stream (either $j= 1$ or 2) entering and leaving the system under isobaric conditions. There is a specific situation where there is a single-phase fluid in a heat-exchanger. In this case we can rewrite 3.2 into

$$q = q_j = \dot{m}_j \Delta h_j = (\dot{m}c_p)_j \Delta T_j \quad (3.4)$$

In this case it is possible to calculate the heat exchange between the two fluids taking into considerations the mass flow \dot{m} and the specific heat at constant pressure c_p of the studied fluid as well as the temperature difference of the studied fluid ΔT_j .

Equation 3.3 reflects a convection– conduction heat transfer phenomenon in a two-fluid heat exchanger. The heat transfer rate is proportional to the heat transfer area A and mean temperature difference ΔT_m between the fluids. This mean temperature difference is a log-mean temperature difference (for counter-flow and parallel-flow exchangers) or related to it in a way that involves terminal temperature differences between the studied fluids.

The coefficient of proportionality U in 3.3 is the overall heat transfer coefficient. Solving a design problem means either determining A (or UA) of a heat exchanger to satisfy the required terminal values of some variables (the sizing problem), or determining the terminal values of the variables knowing the heat exchanger physical size A or overall conductance UA (the rating problem) [16].

Considering the previous information, regarding the quantitative point of view heat exchanger design methodology, there are several paths to solve the heat exchanger thermal design problems. Among all, the most important ones are the rating and the sizing prob-

lems.

The rating problem is based on taking an already existing heat exchanger and analyze the heat transfer and pressure drop of this already existing device. This analysis is called the rating problem. Inputs to have into consideration for this problem are the construction type, flow arrangement and overall dimension, materials, Re and Nu numbers, fluid flow rates and inlet temperature. Using this information of the already built-up heat exchanger, the aim is to determine as output variables are the fluid outlet temperature, total heat transfer rate and pressure drop on each side of the heat exchanger.

The sizing problem, nevertheless, deals with the selection of an exchanger construction type, flow arrangement, tube/plate and fin material, and the physical size of the exchanger to meet the specified heat transfer and specified pressure drop requirements. This problem is also known as a design problem. There are several known methods for carrying out this sizing problem called -NTU method, P-NTU method and MTD. Each of them represents the heat exchanger effectiveness, temperature effectiveness and the mean temperature difference respectively. These will be computational based methods used to complete the sizing problem for the design of a new heat exchanger. They are complicated methods and, as the scope of this project does not cover the design of a heat exchanger, they are only going to be mentioned. More than 65% of the market share is held by shell and tube heat exchanger, due to: versatility of operating in a wide range of conditions using different materials, design experience of more than 100 years and proved design method that actually work efficiently.

For this reason, the components-parts of this type of heat exchanger are going to be outlined in the following lines:

- Tubes: The selection of the tube material and dimension is crucial as the heat exchange takes place across the tubes. In most occasions plane tubes are used for the design; however, in some applications finned tubes are used so as to encourage the heat transfer. According to the experience, small-diameter tubes are more efficient with higher heat transfer rates and more compatibility.
- Tube Pitch and Layout: This is a relation between the distance between tubes (pitch) and each diameter. In most shell-tube exchanger the ratio between tube pitch and the diameter goes from 1.25 to 2. The layout or configuration of these tubes also varies, having triangular or square format as preferred layouts.
- Baffles: They are special plates inside the shell that have the aim to control the overall fluid direction inside the shell. They not only control the direction and support the tubes, but baffles increase turbulence as well, allowing a better heat transfer between the fluids.
- Shells: This is the case where the rest of the elements are placed. There are 7 types of shells and each of them are selected depending on the type of fluid, tube arrangement and according to the expertise.
- Front-end heads and rear-end heads: They are placed in each of the sides of the heat

exchanger. The major criteria of the selection of these parts are the the thermal stresses, operating pressures, cleaning, hazards, and cost.

3.1.1.3 Electric Heater

Water electric heater is the third important element of the set-up. This device is responsible for heating-up the water by using the auxiliary 240V electric power. Actually, there are two types of heaters in the industry: the gas heater and the electric heater. It is possible to classify these heaters in tank heaters and tankless heaters.

The difference in the second classification is really obvious. We use a tank to keep hot water there without the necessity to reheat it and we use the tankless option to have instantaneous hot water instantaneously. The advantages of the tankless heater are the following[21]:

- Endless hot water: There is no possibility of running out of hot water, while in the tank heater, it is a must to wait for the tank to refill.
- Efficiency: It is more efficient regarding the waste of power, as in this case we use the electric power just when it is needed .
- Size and place: The heater is really compact even though it is really powerful. There is no need to have the auxiliary tank so we save that space.

Classification of Heaters

Regarding the classification of gas or electric heaters the following comparison could be done:

Gas water heaters are not 100% efficient and need to have a chimney to evacuate the gases. There are eventually some highly efficient gas heaters which do not require a chimney. However, they require a system composed by a fan and a pipe to evacuate these gases. This problem regarding the gases does not happen in the electric heater.

Electric heaters use electric coils to warm up water. They are cheaper and easier to install. Nevertheless, the problem deals with the electricity costs as the electricity is overall more expensive than the natural gas. These electric heaters are more accurate to heat up less volumes of water while gas heaters have a much faster recovery rate, ideal for bigger water volumes[5]. We are going deeper on the electric water heaters, although the functioning of both of them is similar. The only difference is the heating process. The electric water heater follows the next steps to heat up water:

The electric heater brings cold water in through the dip tube and it heats up using the coil resistance inside of the tank. The hot water rises in the tank and it is moved out thorough the heat-out pipe. The electric power heater has a thermostat, temperature and pressure relief valve, a drain valve, tank insulation and an anode rode. This last one is to deal with corrosion effect. The water is heated by a 240V external electric supply[28].

3.1.2 Secondary elements of the set-up

Throughout this section, the actual elements of the set-up are going to be explained. These elements, with the exception of the electric valve and the pipe, are not going to be modelled. Therefore, a deeper explanation of the actual elements is going to be done in order to facilitate the understanding of the full set-up. Here there are all the secondary elements listed as well as a short description of each of them:

- Pipes: The pipes are the joining elements that will connect all the principal and secondary elements. They are all copper pipes with 10mm diameter and a thickness around 1mm. The roughness of the pipe is $\approx 0.015\text{mm}$ and this roughness depends only on the material, in this case new copper.
- Electric valve: This valve is used to limit the fluid that comes from the pump. The principal objective of this valve is to help the pump reduce the flow below 7 l/min, as this is the minimum pumping flow of the pump. The electric valve is electrically controlled with an analog signal which goes from 2 to 10 V. The control speed is 10 s/mm and the total stroke is of 6.9 mm.
- Ball Valve: The set-up is full of manual ball valves. These valves are different to the electric ones in two ways: the valves cannot be controlled and are opened or closed manually; and these valves allow the flow of water or they cut completely the flow, they do not have the ability to cut the half of the flow. The flow is cut off by a spherical ball inside the valve that interrupts the flow of the water.
- Accumulator: This is a device that keeps the water pressured due to a nitrogen chamber. This device permits to have water pre-pressured before entering the hydraulic circuit to be absorbed by the pump. This pre-pressurization helps the pump because the effort made by it is lower due to this initial accumulator help. The accumulator does not need additional energy supply as the gas does this work.
- By-pass: This is a security device that avoids over-pressures inside the system into the heat exchanger and allows to by-pass part of the flow out from the heat exchanger. It can be regulated from 1.5 to 3.5 l/min and this measure is read by the rotameter installed in this device. This rotameter is a type of flowmeter that permits us to read the actual flow across the by-pass.
- Sensors: There are 3 types of sensors that measure temperature, pressure and flow in different points of the hydraulic circuit. These sensors will be deeply explained in further chapters. They give us the necessary information for the experimental measuring results.
- Quick connectors: These connectors enable to easily plug in-out the electric heaters with the rest of the set-up.

3.2 Creation of Models

The modelling stage is crucial in order to compare it with the real device. The idea is to make two different model. On the one hand, we are looking for a purely theoretical model where the results are obtained by mathematical calculations. In this case, we have chosen the Maple software. On the other hand, we are looking for a model for real simulation and for this stage, the software chosen has been Matlab. Inside this software there is a particular package called Simscape that allows us to use physical models to build up our model.

The model's aim is to calculate the pressure drop of the heat exchanger, and compare it to the real set-up. Basically, this model is based on the fluid mechanics theory. Bearing in mind the theoretical information mentioned throughout the previous chapter and the different components of the set-up, the elements that will be modelled are the pump, the heat exchanger and the pipes. On this point, it is important to work with real specific elements instead of general ones. For this reason, here are explained the 3 specific elements we have used in the set up.

- Grundfos, 98389685_CRE_34_AA AEHQQE: This is the specific pump used in the set up. It is a vertical, multistage centrifugal pump with integrated frequency converter.
- Güntner, flat compact GFHC: It is a shell and tube cross flow flat heat exchanger. It has a fan in the upper part to help air flow through the tubes and optimize the heat exchange through forced convection.
- Copper tubes: These new copper tubes connect the different devices of the set up.

For the pressure drop analysis of the system, therefore, first of all a theoretical analysis will be done to understand the the different steps done to achieve the objective.

3.2.1 Fluid mechanics pressure drop theory

For the pressure drop analysis of the system, the basic theory will be next explained based on the fluid mechanics analysis. The two different models that are going to be later explained are based on this theory.

This analysis will consist of an energy balance of the system, always between two known hydraulic points. The total energy per mass unit in a given point in a fluid flow consists of elevation (potential) energy, velocity (kinetic) energy and pressure energy. The Energy Equation states that energy can not disappear - the energy upstream in the fluid flow will always be equal to the energy downstream in the flow and the energy loss between the two points [27].

$$\frac{P_1}{\rho g} + \frac{u_1^2}{2g} + h_1 = \frac{P_2}{\rho g} + \frac{u_2^2}{2g} + h_2 + \Delta H_{1-2} \quad (3.5)$$

Some assumption will be done on this point to avoid complex calculations. Regarding the 3 energetic elements, we can assume that the elevation is going to be negligible as the set-up elevation difference are little and we can consider that we are operating in a straight line.

At the same, baring in mind that the diameter of the tube is constant, and according to the continuity equation

$$\dot{Q} = uS \quad (3.6)$$

The velocity u only depends on the cross section S of the pipe and the volumetric flow \dot{Q} . As \dot{Q} is constant for flowing in a single line and as there is no change in pipe diameter, we can assume that there is no a significant change in u of the two different points. Therefore, the final energy balance will be the following

$$\frac{P_1 - P_2}{\rho g} = \Delta H_{1-2} \quad (3.7)$$

This new equation states that the total energy losses ΔH_{12} depend only on the pressure drop of the system. We can rewrite this expression on the following way

$$\frac{\Delta P}{\rho g} = \Delta H_{1-2} \quad (3.8)$$

The objective, therefore, will be calculate this energy losses, that from this point on, are going to be named as pressure losses or pressure drop.

First of all, what pressure is will be defined. Pressure drop is defined as the difference in total pressure between two points of a fluid carrying network. This decrease in the pressure of the fluid occurs due to frictional forces basically as the fluid flow through the pipe, causing a resistance to the fluid flow. The main determinants to this change in pressure are the fluid velocity and the fluid viscosity as well as the pipe characteristics [27].

The head loss of a pipe, tube or duct system, is the same as that produced in a straight pipe or duct whose length is equal to the pipes of the original systems plus the sum of the equivalent lengths of all the components in the system. This can be expressed as

$$h_{loss} = h_{major_loss} + h_{minor_loss} \quad (3.9)$$

Where h_{loss} is the total pressure drop in the pipe system. The factors h_{major_loss} and h_{minor_loss} refer to the major and minor pressure losses respectively. Major pressure loss is related to the friction in pipes while minor pressure loss is related, instead, to valves or change in direction of the pipes, such as, elbows. This affirmation could also be described in a mathematical way, as it follows

$$h_{major_loss} = \frac{\lambda L}{d} \frac{u^2}{2g} \quad (3.10)$$

This equation states the major head loss and it is a relation among the geometric and flow characteristics and λ known as the friction factor characteristic from the pipe.

$$h_{minor_loss} = \xi \frac{u^2}{2g} \quad (3.11)$$

This other equation refers to minor losses and it varies with the constant ξ that is ranged from

0 to 1, depending on the minor loss type. These constants are tabulated by experimental research. Actually, the minor losses are commonly neglected due to little effect they have regarding to the major ones and even more in a big set-up as the one we are handling.

For this reason, the final expression we are going to use to define pressure drop from this point on is the following

$$\Delta P = \frac{\lambda L u^2}{d 2g} \quad (3.12)$$

known as Darcy-Weisbach equation. This is the expression used for calculating the difference in pressure between two points in a pipe or in a conduct.

Once the objective equation is clear, we should state which is the procedure that should be followed to achieve the different values which conform the equation. Geometrical values will normally be known including the cross section d of the pipe known as hydraulic diameter and the length L of the pipe. For a tubular pipe this d is equal to the diameter of the pipe and the L is the distance between the two studied points. Gravity g will always be a constant, therefore the variables we need to calculate are the velocity u of the fluid and the friction factor λ [27].

Obtaining the velocity of the fluid u is dependant on the volumetric flow of the studied fluid and the cross section of the pipe or conduct. This relation could be justified by the already shown continuity equation 3.21.

Regarding the friction factor λ depends on the type of flow, being laminar, transient and turbulent and on the relative roughness of the pipe ϵ . Flow is defined by the Reynolds number. The Reynolds number is the ratio of inertial forces to viscous forces. It is a dimensionless number used to categorize the fluids systems in which the effect of viscosity is important in controlling the velocities or the flow pattern of a fluid[19]. Mathematically, the Reynolds number, Re , is defined as

$$Re = \frac{\rho u D}{\mu} \quad (3.13)$$

where:

- ρ fluid density
- u average velocity
- D pipe internal diameter
- μ dynamic viscosity

The Reynolds number is used to determine whether a fluid is in laminar, critical and turbulent flow. This critical area is an intermediate area where the actual flow behavior of the fluid is not defined, so, regarding the calculations this critical zone is often not considered or adapted to one or the other known areas. Therefore, it is assumed that a Reynolds number less than or equal to 2100 indicates laminar flow, and a Reynolds number greater than 2100 indicates turbulent flow. The friction factor λ of the pipe, indeed, depends on the type of flow determined by the Reynolds number. There are several different ways to calculate this λ , however, those could be summarized into analytical or graphical way. Regarding the

graphical way, the determination of the λ is determined by the Moody chart. This Moody chart is a non-dimensional form that relates the friction factor λ from Darcy Weisbach equation 3.18, N_{Re} and relative roughness of the pipe ϵ/d for fully developed flow in a circular pipe [6]. The way to look for λ value in the table is first of all defining the Re number and define the type of flow that is flowing through the pipe. Besides, it is important to know the material of the pipe because this will make an impact on the ϵ of the pipe and, therefore, on λ . Having into consideration these two variables, it is possible to obtain from the chart the friction factor λ .

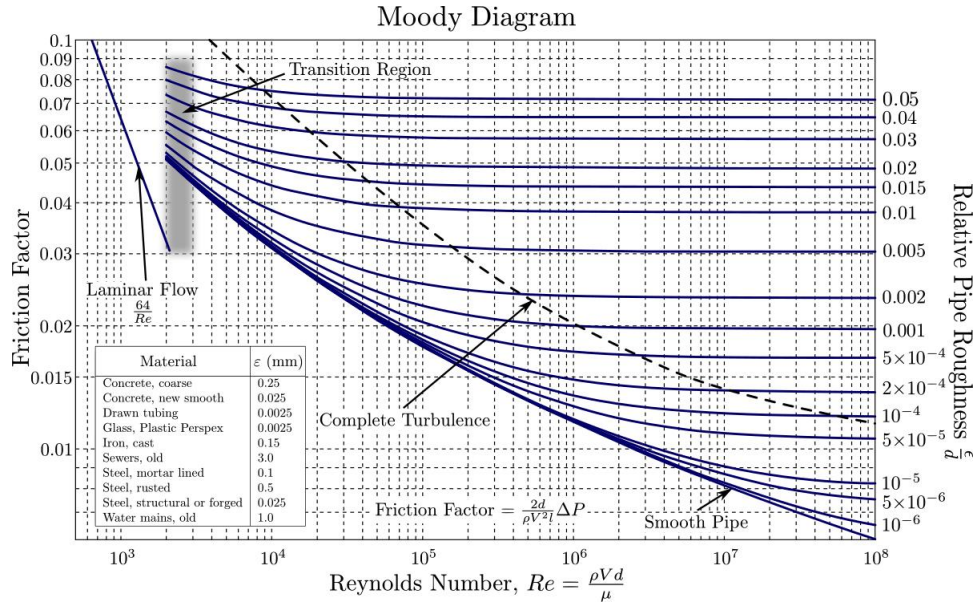


Figure 3.5: Moody Diagram
[6]

In principle Moody diagram 3.5 is used for solution of three types of problems, i.e. problem in which head loss is unknown, in which volume flow rate is unknown and in which diameter is unknown [2]. According to 3.5 we notice that in the laminar flow region, the correlation between Re and friction factor λ is linear and non-dependant on the relative roughness ϵ/d of the pipe. For this reason, when the Re is below 2100, λ will be calculated by

$$\lambda = \frac{64}{Re} \quad (3.14)$$

In the case the flow is turbulent, the friction factor λ will be the result of combining on the chart the Reynolds number N_{Re} and the relative roughness ϵ/d of the pipe.

Another option is instead of obtaining λ by using the Moody Chart 3.5, is by using an analytical way. There are several correlation through a wide variety of bibliographies that include different ways of obtaining the friction factor using an analytical correlation. These correlations had been obtained by experimental analysis. Among these different correlations, the most important ones are the following [2]

$$\frac{1}{\sqrt{\lambda}} = -2 \log_{10} \left(\frac{2.51}{Re\sqrt{\lambda}} + \frac{\epsilon}{3.71D} \right) \quad (3.15)$$

Colebrook equation 3.15 describes a monotonic change in the friction factor from smooth to fully rough. It is valid especially for commercial steel pipes. How well Colebrook equation fits the experimental data is beyond the scope of presented approximations. Perhaps one of the following equations even fits the available data better than the Colebrook equation. Until the comparison is made with real, measured values, however, this will not be known. There are over 20 different approximations to estimate this correlation. Among these expressions, one of the most used one is Haaland approximation due to its accuracy and simplicity. This expression is given as it follows:

$$\frac{1}{\sqrt{\lambda}} = \frac{-1.8}{n} \log_{10} \left(\frac{\epsilon}{3.71D}^{1.11n} + \frac{6.9^n}{Re} \right) \quad (3.16)$$

For n=1, Haaland equation 3.16 is valid for flow of liquid. Haaland suggested that n=3 yields friction factors in consonance with those recommended for use in gas transmission lines [2]. For this reason from this point on, as long as we are working with fluids, we could rewrite 3.16 as

$$\frac{1}{\sqrt{\lambda}} = -1.8 \log_{10} \left(\frac{\epsilon}{3.71D}^{1.11} + \frac{6.9}{Re} \right) \quad (3.17)$$

Estimated error of approximation by Haaland valid for liquid flow is up to 1.4% compared with implicit Colebrook equation. Having into consideration this last expression, the requirements to calculate λ , are the same as in the Moody Chart 3.5: Re and ϵ . Once these variables are known, it is possible to calculate the searched pressure drop by applying Darcy Weisbach equation 3.18.

Once the theoretical explanation of the calculation of the pressure drop is done, throughout the following chapters two different models of the set-up pressure drop calculation will be done.

3.2.2 Mathematical based model

Mathematical based model will be explained using Maple software. We are going to base this explanation on 3.2.3 as it will be followed literally the theoretical part to make the necessary calculation to overcome the desire results. According to the simplifications made in the section 3.2.3, we are going to start introducing the model we are going to make the calculations about.

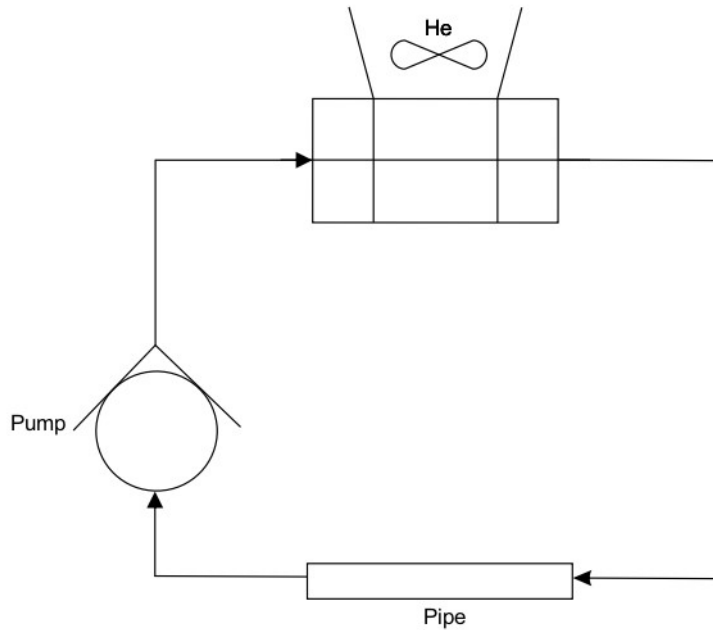


Figure 3.6: Mathematical simplified model

In the picture 3.6 we can see a combination of the three elements that are going to be studied. The decision of including only these elements is based again on the section 3.2.3. We have eliminated elements such as the valve that will cause a minor pressure drop, when it is completely open, or all the minor pressure drops that come from the different change in direction of the pipes. The analyse will be based only on the major pressure drop and, due to this, the simplified model includes the heat exchanger, the pump and a pipe that will have the same length as the sum of the total length of the different pipes.

Due to the presence of only major losses, we can base our calculation in resolving Darcy Weisbach equation 3.18. It is better to remember it once again, as this chapter will be based on the calculation of this expression.

$$\Delta P = \frac{\lambda L u^2}{d 2g} \quad (3.18)$$

As already mentioned, this pressure drop result will be based on the calculation of the velocity u and the friction factor λ . These two calculations will be done separately. Before

starting with the calculations, the necessary different variables will be listed with their respective units for solving the mentioned formulas. Furthermore, some problem data is already known and this will be also listed to focus only on the unknowns.

Pressure drop problem variables and units		
Symbology	Description	Units
ΔP	Pressure drop	m
λ	friction factor	-
\dot{Q}	fluid volumetric flow	m/s^2
u	fluid velocity	m/s
D	diameter	m
g	gravitational acceleration	m/s^2
L	Pipe equivalent length	m
Re	Reynolds dimensionless number	-
ρ	fluid density	kg/m^3
μ	fluid dynamic viscosity	$Pa * s$
ϵ	Pipe absolute roughness	m

Table 3.1: Pressure drop problem variable description and units

At the same times, some of these variables could be onsite measures, such as, geometric variables. Besides, fluid property variables, which depend on the temperature of the fluid, are also tabulated and are not going to be unknowns for us. For this reason, here we have the following table where we can find the problem data, with the units shown in the table 3.1:

Pressure drop problem data	
Variable	Numerical Value
D_{He}	0.02 m
D_{pipe}	0.028 m
L_{He}	90 m
L_{pipe}	12 m
$\rho_{water(20C)}$	998.2 kg/m^3
$\mu_{water(20C)}$	$1.002 * 10^{-3} Pa * s$
ϵ_{copper}	$0.002 * 10^{-3} m$
g	$9.81 m/s^2$

Table 3.2: Pressure drop problem data

Once the problem data is clear, we realize that the first step (calculation of u) using the continuity equation 3.21 is not direct, as we lack of the volumetric flow \dot{Q} . This will be the first step of this analytical problem, known as the operation point (OP) calculation.

3.2.2.1 OP calculation

The operation point will be the point where the pressure given from the pump to the fluid equals the pressure drop caused in the system. Therefore, the power that the pump gives to the fluid is completely used by the system without having excess of power. By calculating this point, the idea is not wasting the power given by the pump and taking advantage of it to cause the heat exchange in the HE. OP will be calculated using both curves; on the one hand the pump characteristic curve that will give us information about different operation points of the pump for several volumetric flows; on the other hand, there will be the curve of pressure losses regarding a combination of the pipe and HE model. The goal is the pressure loss in the HE to be maximal and greater compared to the pipe pressure losses, as they are real losses and cannot be used.

For the pump characteristic curve we have based our calculations on the manufacturer curves.[14]

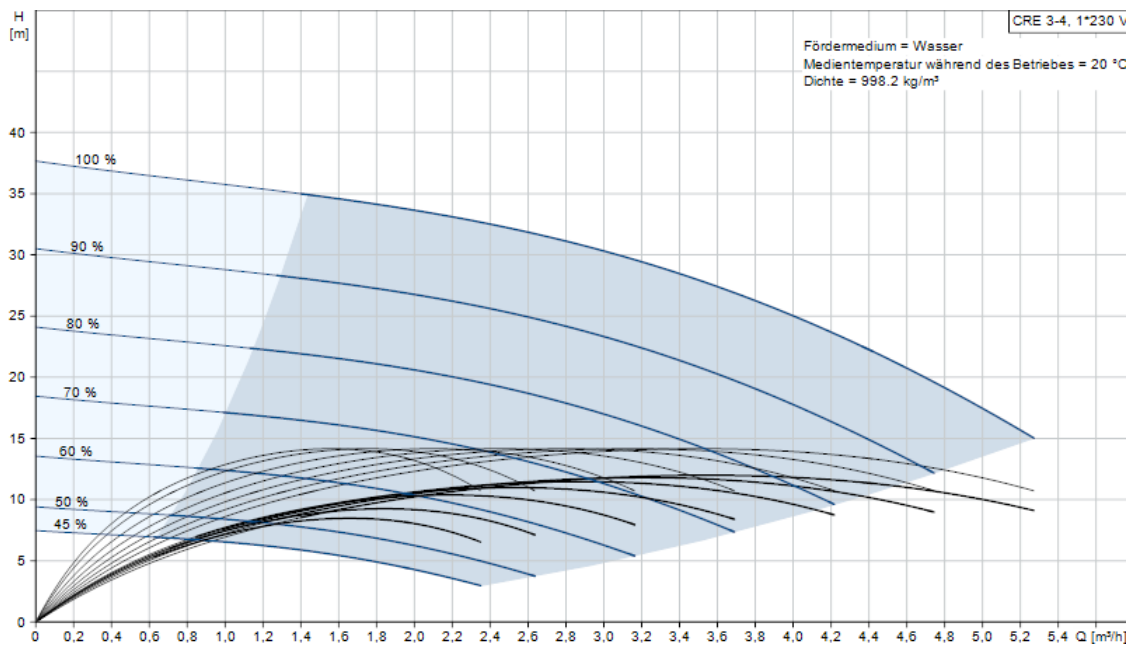


Figure 3.7: Grundfos pump characteristic Curves [14]

These curves have been the orientation model to understand how Grundfos pump works. In 3.7 different pump characteristic curves are shown regarding different $\%$. These different $\%$ make reference to the pump rotational speed being the 100% the maximum rotational speed of the pump.

We decided to make some experiments first to calculate the pressure the pump gives to the fluid in different points. We found out that we have a limitation due to the volumetric

mass flow, as it is limited to 25 l/min. Therefore, it has not been possible to work with the 100% of the pump power due to this limitation. After doing some experiments and taking some flow-pressure experimental points, we saw that the the characteristic curve we were moving across was the 60% one and that is the one we are going to use to find out which is the OP.

Having clarified which is going to be the curve we are going to base our calculations on, there will be two approaches done to have the best model. On a first approach, the idea was to make a linearized model of this curve in order to simplify the calculations. Afterwards, this linearized model would be compared and contrasted with the real model[17] of the pump curve. According to the 60% curve on 3.7, these are the linearized and real mathematical models of the pump characteristic curve, respectively:

$$\Delta P_{pumplinearized} = \frac{(-2.7(\dot{Q} * 3600) + 18.3)\rho g}{10^5} \quad (3.19)$$

$$\Delta P_{pumpreal} = \frac{\Delta P_0 \left(1 - \frac{\dot{Q}^2}{\left(\frac{\dot{m}_0}{\rho}\right)^2}\right)}{10^5} \quad (3.20)$$

It is important to make a clarification regarding the units we are going to use and the respective unit conversion associated to these units. The units used to the variables and constant inside these equations are the following:

Units and values of the variables and constants		
Variable	Value	Unit
Pump pressure drop ΔP_{pump}	-	bar
Volumetric flow \dot{Q}	-	m ³ /s
Constant	Value	Unit
Reference pressure drop ΔP_0	1.3*10 ⁵	Pa
Reference mass flow \dot{m}_0	1.2	kg/s

Table 3.3: Variable and constants characteristic curve units and values

At the same time, inside the formulas 3.19 and 3.20, there have been already conversion unit parameters implemented and it is important to clarify them in order to understand and manage to differ between the components of the equation and the conversion factors.

Conversion factors		
Unit	Conversion factor	Unit
m	ρg	Pa
Pa	$1/10^5$	bar
m^3/h	$1/3600$	m^3/s
kg/s	ρ	m^3/s
m^3/s	60000	l/min

Table 3.4: conversion factors

It is important to highlight the reason of these conversion factors. First of all regarding

3.7 we can see that the units are m and m^3/h for pressure and flow, respectively. The line has been modelled according to those units and afterwards reconverted to the units we are looking for. At the same time, the constants used have their own units assigned, therefore it is important to make the required changes. To finish with, from this point on and to have a better understanding of the results showed in the following pages, the units we are going to use are *bar* and *l/min*. Table 3.4 is going to be guide for the user in order to understand in every moment the conversion done regarding the unit system.

Once the equation of the pump is clear and \dot{Q} dependant, the goal for both, pipe and HE is having in both cases a expression \dot{Q} dependant as well. For doing so, we are going to base the calculation again on the Darcy Weisbach 3.18 equation. The problem is identical as in the previous case; Nevertheless, having as unknowns u and λ , the aim is to have both variables \dot{Q} dependant. 3 expressions are going to be necessary to reach the objective: Continuity equation 3.21, Haaland aproximation 3.22 for calculating the friction factor and the Reynolds number 3.25 included in the 3.22. Combining these 3 equations, a unique expression \dot{Q} dependant will be obtained. Find below the 3 mentioned equations in order to clarify the process.

$$\dot{Q} = uS \quad (3.21)$$

$$\frac{1}{\sqrt{\lambda}} = -1.8 \log_{10} \left(\frac{\epsilon}{3.71D}^{1.11} + \frac{6.9}{Re} \right) \quad (3.22)$$

$$Re = \frac{\rho u D}{\mu} \quad (3.23)$$

The combination of this 3 equations will give as a result a expression based on pressure drop Darcy Weisbach 3.18

Using the potential of Maple and equalling the pressure drop of the modelled elements using both linearized and real pump cases as it follows

$$\Delta P_{pump\ linearized} = \Delta P_{HE} + \Delta P_{pipe} \quad (3.24)$$

$$\Delta P_{pump\ real} = \Delta P_{HE} + \Delta P_{pipe} \quad (3.25)$$

The first step, indeed, should be selecting the best model between these two. For doing so, both models will be compared to the manufacturer curve showed in 3.7.

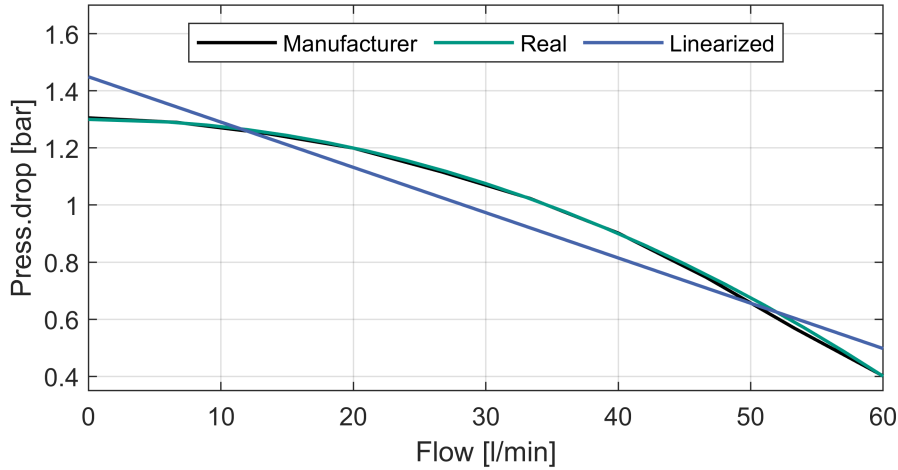


Figure 3.8: Comparison between the real and linearized curve with manufacturer's curve

According to the figure, we can see that the linearized model causes a big error in the approximation, and that the real curve fits almost perfectly to the manufacturer's curve. For this reason we are going to pursue the real approximation to calculate the OP of our system.

Once we have decided to use the real characteristic pump curve, we need to compare it with the curve of pressure drop of the system. In this case, we are going to consider a combination of the pressure drop of the pipe system and the heat exchanger. This curve has been obtained as a result of the combination of the mentioned 3 equations. The idea is to look for the optimal point, OP, where the power the pump gives to the fluid will be completely exhausted in the system.

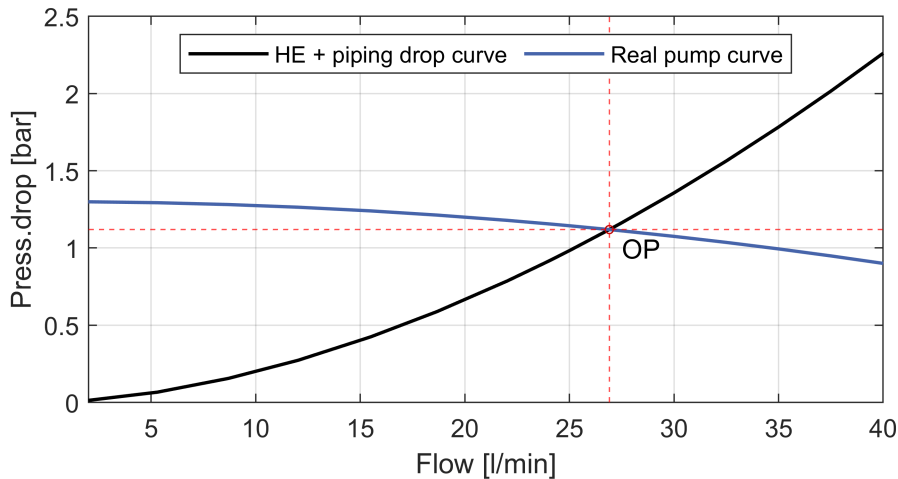


Figure 3.9: OP

OP	
Flow [<i>l/min</i>]	Pressure drop [<i>bar</i>]
26.907	1,119

Table 3.5: OP

According to this graphic, we notice that the theoretical OP is above the 25 l/min which is the limit of the flow sensor. This only means that we need to work below the optimal potential of the pump because we are not able to measure that flow (although the pump has enough power to achieve that point). It is important to see how far from the OP we are going to work using this 25l/min volumetric flow.

Ideal OP and working OP		
Pump dp	Pipe+HE dp	ΔP
1.119	1,119	0
1.143	0,983	0.16

Table 3.6: OP error

According to this comparison, we can appreciate that the working point is not going to be far away from the actual OP point. The loss is going to be of 0.16bar, which is more than assumable. Therefore, once we have accomplished the objective of calculating the OP and having established the working volumetric flow, we are going to move on the results section

3.2.2.2 Maple pressure drop results

In this chapter we are going to see calculation of the results of the pressure drop for different volumetric flows. The goal of these calculations is seeing the impact of the piping system comparing to the HE and the effect of going far from the OP. Calculation regarding the pipe system and HE pressure drop will be done combining the 3 mentioned expressions: Continuity equation 3.21, Haaland approximation 3.22 and the Reynolds number 3.25 included in the 3.22. At this point, the volumetric flow is no longer a variable, therefore, the calculation is direct. The results obtained in Maple are the following.

Pressure drop results obtained on Maple				
	ΔP Pressure drop [bar]			
\dot{Q} flow [lpm]	Pipe	HE	HE+Pipe	Pump
1.90	0.0003	0.012	0.0127	1.299
5.3	0.002	0.065	0.067	1.293
8.7	0.004	0.152	0.156	1.281
12.03	0.007	0.266	0.273	1.264
15.5	0.011	0.414	0.425	1.240
18.67	0.016	0.572	0.588	1.213
22.03	0.0213	0.766	0.787	1.179
25	0.0263	00.957	0.983	1.114

Table 3.7: Pressure drop results obtained on Maple]

According to these results, it is really relevant the comparison between the piping pressure drop and the HE one. In fact, we can say that we can neglect the effect of the pipe system comparing to the HE one. Besides, we can see that when we go far away the OP, the pump power wasted increases a lot. Therefore, we can conclude that we need to work near the OP in order to make a good use of the pumping power.

3.2.3 Simulation based model

Having done a theoretical model, it is necessary to compare it with a simulation model so as to understand the real time behavior of the set up. The model will be done on Matlab Simscape.

The very first attempt is deciding which are the key elements which should be modelled. Once again the elements we are going to work with are the pump, the HE and the pipping system. The aim of this chapter is to explain step by step how it has been done the complete modelling of the set-up, starting for the separate elements, into the complete model. To finish with this chapter, the obtained results will be showed. To have an overall view of it, here we can see a simplified model of the full model used to run the simulations.

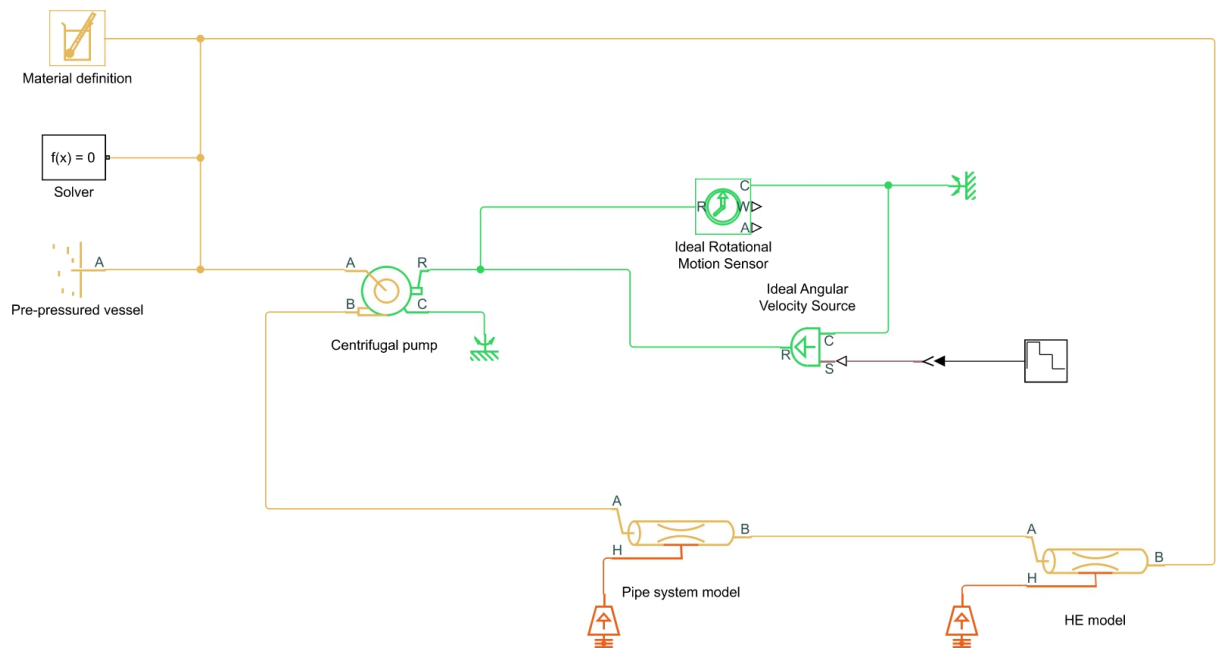


Figure 3.10: Matlab Simscape full model

In this model all the measurement equipment is missing. Nevertheless, all the required components to run the simulation are included, among them, the pipe system, pump and HE complete models. These elements are going to be in detail described in the following sections.

3.2.3.1 Model parameters

This model has been constructed in terms of reliability, precision and computational cost. The model only considers the pressure drop influence due to major pressure losses. Temperature change will be neglected as the heaters are switched off for this experiment. It is possible to have a little temperature increase due to the effect of the pressure losses, affecting the density ρ and the dynamic viscosity μ . Actually, this difference is tiny and it does not affect to the calculations of the pressure drop. Baring these little insights in mind, through this section the model is going to be in detail explained, showing a detailed parameter selection to achieve the most effective and reliable model.

Pump model

To begin with, we need to recall the type of pump we are working with. The Grundfos pump we are working with is a centrifugal vertical pump. The pump being vertical of the pump does not affect to the modelling as it only affects to the direction of the water on the intake area. We are going to select the centrifugal pump element inside the library browser. The very first step is setting the parameters we are going to work with.

In the first row, we need to make an important decision that will condition the rest of the parameterization. In this case, making use of the manufacturer data, a 2D parameterization will be done. The idea is to take from the different manufacturer characteristic curves 3.7, the required data to complete a 2D table as an input for Matlab Simscape centrifugal pump. The aim is to model both the head $H[m]$ and the pump's brake power W_b according to the flow \dot{Q} and the angular speed $\dot{\omega}$ of the pump. According to the collected data, here we can see the parameterization of both variables, as explained.

2D parameterization head $H[m]$				
	$\dot{\omega}$ angular speed vector [rpm]			
\dot{Q} flow vector [lpm]	1500	2100	2800	3500
8.67	7.098	12.54	23.87	36.75
16.67	6.825	12.36	23.42	35.9
25	6.009	11.9	22.43	34.91
33.33	5.193	11.27	19.84	33.49
41.66	3.379	9.365	19.25	32.35
50	2.443	2.993	17.8	30.7

Table 3.8: Head $H[m]$ table $[\dot{Q}, \dot{\omega}]$ parameterization

2D parameterization brake power $W_b[kW]$				
	$\dot{\omega}$ angular speed vector [rpm]			
\dot{Q} flow vector [lpm]	1500	2100	2800	3500
8.67	0.027	0.055	0.132	0.238
16.67	0.036	0.074	0.166	0.28
25	0.043	0.091	0.192	0.328
33.33	0.051	0.109	0.203	0.369
41.66	0.052	0.114	0.232	0.409
50	0.057	0.116	0.258	0.432

Table 3.9: Brake power $W_b[kW]$ table [$\dot{Q}, \dot{\omega}$] parameterization

Having clarified these 2 parameterization tables, 3.16 and 3.9 with data taken from manufacturer characteristic curves 3.7, the pump is practically completely parameterized. Having done a 2D parameterization permits the pump to be much more in detail explained and allows Matlab Simscape to make the best use of this block. Additionally, besides this data, other parameters should be added and could be seen in the following table.

Centrifugal pump parameters		
Parameter	Value	Unit
Mechanical orientation	positive	-
Reference density ρ	998.2	kg/m ³
Angular speed treshold for reversal ω_{rev}	10	rpm
Cross section area of connecting pipe	0.01	m ²

Table 3.10: Centrifugal pump rest of the parameters

This parameterization should be sufficient to define the pump hydraulically. Nevertheless, the mechanical part of the pump should be modelled as well. For the rotation of the shaft, an ideal angular velocity source and a mechanical rotational had been added in the ports R and C of the centrifugal pump respectively. For the angular velocity sensor, it is important to add an input signal to parameterize the rotational speed. In this case, different options are available. A constant could be added if the idea is to simulate only an specific OP or instead, a variable input signal could be added in order to study different OP.

To finish with, it is important to control and monitor the motion of the pump. For doing so, an ideal rotational motion sensor has been connected to the ideal angular velocity source. This full explanation is graphically explained in the next figure.

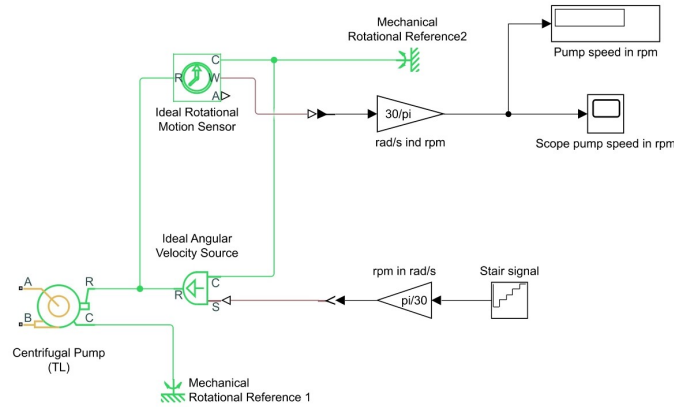


Figure 3.11: Matlab Simscape Grundfos pump model

HE and pipe model

The same section will be defined to explaining both models, the HE and the pipe system. Although they are completely different elements, actually they could be modelled in the same way. Both of them could be modelled as a unique pipe with a diameter and length equivalent to the elements.

For modelling both elements, therefore, a Pipe will be selected from the library browser inside the elements of the thermal liquid library. The parameterization that should be done is explained in the following tables for each of the elements.

Heat Exchanger parameters		
Geometry		
Parameter	Value	Unit
Pipe length	90	m
Cross sectional area	0.000314	m ²
Hydraulic diameter	0.02	m
Friction and Heat Transfer		
Parameter	Value	Unit
Aggregate equivalent length of local resistances	0	m
Internal surface absolute roughness	0.002*10 ⁻³	m
Laminar flow upper Reynolds number limit	2100	-
Turbulent flow lower Reynolds number limit	2101	-
Laminar friction constant for Darcy friction factor	64	-
Nusselt number for laminar flow heat transfer	3.66	-
Effects and initial conditions		
Parameter	Value	Unit
Fluid dynamic compressibility	off	-
Initial liquid temperature	20	°C

Table 3.11: HE parameterization

Pipe system parameters		
Geometry		
Parameter	Value	Unit
Pipe length	12	m
Cross sectional area	0.00062	m ²
Hydraulic diameter	0.028	m
Friction and Heat Transfer		
Parameter	Value	Unit
Aggregate equivalent length of local resistances	0	m
Internal surface absolute roughness	0.002*10 ⁻³	m
Laminar flow upper Reynolds number limit	2100	-
Turbulent flow lower Reynolds number limit	2101	-
Laminar friction constant for Darcy friction factor	64	-
Nusselt number for laminar flow heat transfer	3.66	-
Effects and initial conditions		
Parameter	Value	Unit
Fluid dynamic compressibility	off	-
Initial liquid temperature	20	°C

Table 3.12: Pipe system parameterization

In both tables we notice that the main difference between the two elements is the geometry part. This geometry part has been on site measured in the set-up using the real devices. It is true that measuring pipe system is easier and has less impact regarding the pressure loss as we saw in the Maple theoretical calculation. Measuring the HE pipe system, however, has been more complicated as we cannot see the inside part of the HE. This measurement has been done calculating the number of tubes and the total length of the HE.

Regarding the friction and heat transfer part, we have to bare in mind that we are neglecting the heat transfer as the effect of this on the pressure drop is barely noticeable. The most important parameters here are the absolute roughness of the pipe and the Reynolds number which will have a notorious effect on the final calculation of the pressure drop. This model is based as well on Darcy Weisbach equation 3.18. Finally, the compressibility of the fluid is negligible as well and will be only considered in case we had a gas as the main fluid.

Once again, in this model we need to complete it with auxiliary blocks for the correct functioning of the system. First of all, we need to attach an ideal temperature source to the pipe. This will be responsible for modelling the thermodynamic part of the pump by assigning a constant temperature. As the temperature input is constant and equal to 20 degC, the effect of the temperature will not be considered for assigning a constant temperature. Furthermore, it is important to obtain data regarding the input and the output points of the pipe. The results obtained here will be the pressure drop we are looking for. To achieve that result, a pressure and temperature sensor will be installed in the output of the pipe, making use of the pressure output only and measuring the difference between the two studied points. It is important to clarify that the fluid in the intake is pre-pressured by the action of the pressure vessel. This means that we are going to do directly the difference between the output and this pressure reference. Having clarified this, here we can see the model of

this equivalent pipe which will be identical for both models.

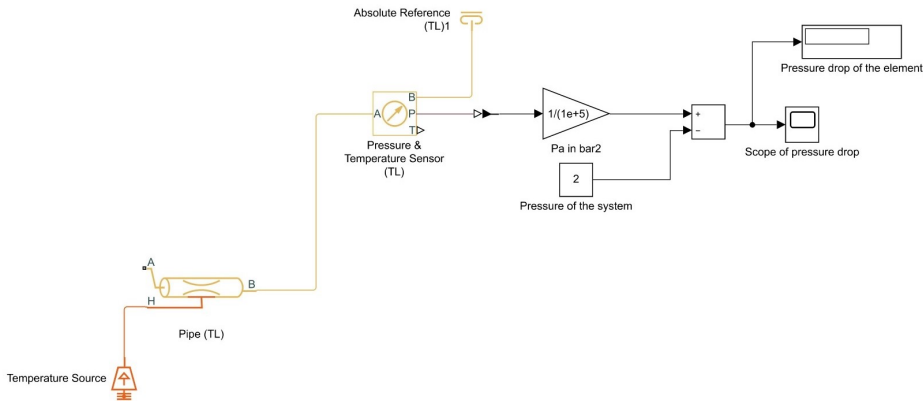


Figure 3.12: Matlab Simscape pipe and HE model

Having clarified the elements that are going to take part in the full model, it is important to show the hole model to understand the connections done between different elements. This full model will be available in the appendix section at the end of this document.

3.2.3.2 Matlab Simscape model results

In this chapter we are going to compare different working OP as we did in the Mathematical calculation chapter. In order to obtain different volumetric flows, we decided to vary the rotational velocity of the pump. This is possible also in the physical set-up and will be explained in further chapters. Therefore, according to different rotational speeds, we are going to obtain pressure drops on the two modelled elements, HE and pipe system. We have already seen that the effect of the pipe regarding the pressure drop is negligible, but we are going to verify it using this model. Before showing the results, it is important to make an annotation because there is a slight difference comparing to the mathematical model. In the mathematical model we obtained directly pressure differences and we used relative pressure; in this model, instead, we use absolute pressure scale and it is important to highlight and to remember that we have pre-pressured water before the pump. This is taken into consideration in the model.

Having clarified this point, this model works exactly the same as the mathematical model as it uses the same theoretical basis.

First of all, we need to calculate the rotation speed to obtain the volumetric flows we calculated in the Mathematical part. We are going to base on the manufacturer's information [14] and we see that the 100% is measured with 3385rpm speed. Based on this calculation and having already calculated the OP, we can know what is the rotational speed that matches that OP.

Having clarified this point, in the next table are shown different pressure drop values for

different rotation speeds of the pump and volumetric flows.

Pressure drop results obtained on Matlab Simscape			
Rotation speed $\dot{\omega}$ [rpm]	\dot{Q} flow [lpm]	ΔP_{Pipe} [bar]	ΔP_{HE} [bar]
689	1.90	0.0002	0.0073
775	5.3	0.002	0.065
894	8.7	0.004	0.153
1043	12.03	0.007	0.267
1228	15.5	0.011	0.415
1436	18.67	0.016	0.575
1684	22.03	0.021	0.769
1915	25	0.026	0.962
2065	26.93	0.029	1.89

Table 3.13: Matlab Simscape pressure drop calculations according to different rotational speeds

In the last line we can see the OP. We can have a reference if it makes sense this speed rotation to the one that is theoretically supposed to be. We know by manufacturers data in [14] that the 100% pump speed is 3385rpm. Taking into consideration that we have used the 60% characteristic curve, this percentage makes reference exactly to the rotational speed. Making the required calculation we are going to calculate how accurate this approximate 60% curve is compared to the model results to obtain the OP:

Pump % comparison model vs Manufacturer curve		
$\dot{\omega}$ 60% manufacturer [rpm]	$\dot{\omega}$ Simscape [rpm]	Error
2031	2065	1.6%

Table 3.14: Comparison OP Simscape model and manufacturer curve

We can see that there is a little error. This error could come due to the manufacturer curve, as it is an approximation taking different point from the graphic available. Nevertheless, we can see that it is a really reliable approximation as well as a reliable model of Grundfos pump as well. Regarding the pressure drop calculation, once again we can prove that the pressure drop from the pipe comparing to the HE one is negligible. These results will be compared in the next chapter to see how accurate is the model to the theoretical results. To finish with the Matlab Simscape model, it is important to show the correlation between the speed rotation $\dot{\omega}$ and the volumetric flow. This correlation will be useful in order to obtain different volumetric flows that are wanted to test in this model. For obtaining this correlation, several points regarding flow and rotation speed have been selected using the Matlab Simscape model. Afterwards, these points have been approximated through a trend curve resulting on this plot.

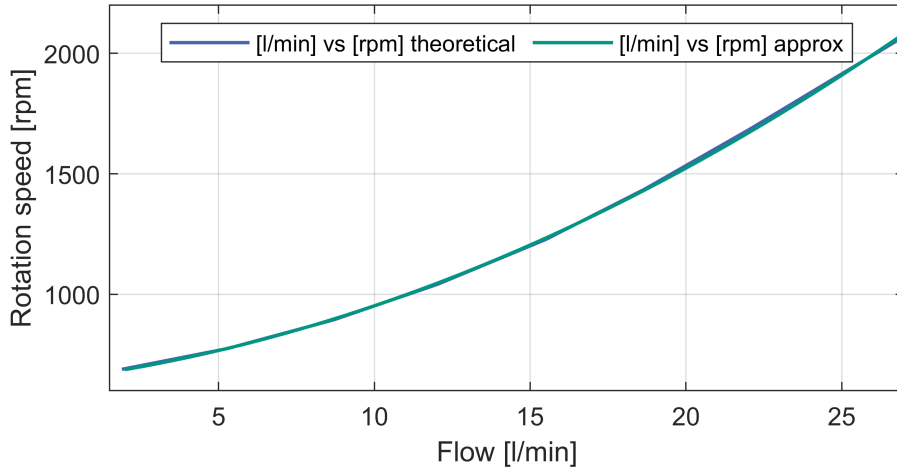


Figure 3.13: Correlation pump rotation speed $\dot{\omega}$ [rpm] and Flow \dot{Q} [l/min] theoretical and approximation

In the figure above, we can see that both curves almost perfectly match. In fact, the theoretical curve has been approximated using a polynomial grade 2 function, being the $R^2 = 0.9998$. This function could be explained as:

$$\dot{\omega} = 1.3345\dot{Q}^2 + 17.114\dot{Q} + 647.62 \quad (3.26)$$

where $\dot{\omega}$ is in [rpm] and \dot{Q} is in [lpm]. This equation will be used in order to know in every OP which is the rotation speed to the pump according to the flow. Besides, not only will be possible to know the exact rotational velocity, but the power % of the pump regarding the maximum power. We need to recall that the pump works with a velocity of 3385rpm in his 100%.

3.2.4 Model and Theoretical Results comparison

Both analysis are completed regarding the mathematical an model based pressure drop calculations. The next step is making a comparison between both models so as to see the real accuracy of the models. The idea is to compare not only numerically, but graphically as well these models and, finally, analyze the deviation between them.

To do so, 2 different tables will be shown in order to compare pressure losses on the piping system and HE.

Pipe system pressure drop results comparison Mathematical and Model			
\dot{Q} flow [lpm]	$\Delta P_{PipeMaple}$ [bar]	$\Delta P_{PipeSimscape}$ [bar]	Error [%]
1.90	0.0003	0.0003	0
5.3	0.0017	0.0018	5.5
8.7	0.0042	0.0042	0
12.03	0.0073	0.0072	1.4
15.5	0.0112	0.0112	0
18.67	0.0155	0.0155	0
22.03	0.0207	0.0207	0
25	0.0258	0.0258	0
26.9	0.0293	0.0292	0.3

Table 3.15: Pipe system pressure drop comparison Mathematical and model and error

HE pressure drop results comparison Mathematical and Model			
\dot{Q} flow [lpm]	$\Delta P_{HEMaple}$ [bar]	$\Delta P_{HEsimscape}$ [bar]	Error [%]
1.90	0.0072	0.0116	37.9
5.3	0.0652	0.0648	0.61
8.7	0.1525	0.1517	0.52
12.03	0.2673	0.2659	0.52
15.5	0.4158	0.4135	0.55
18.67	0.5749	0.5725	0.42
22.03	0.7692	0.7660	0.42
25	0.9614	0.9571	0.45
26.9	1.089	1.090	0.1

Table 3.16: HE pressure drop comparison .Mathematical and model and error

According to the results, the obvious conclusion is that mathematical and model based calculations match. Therefore, we can conclude that the model is reliable and ready to be compared with the experimental results. These results going to be plotted as well, in order to see the real magnitude of the error and be aware of how little it is.

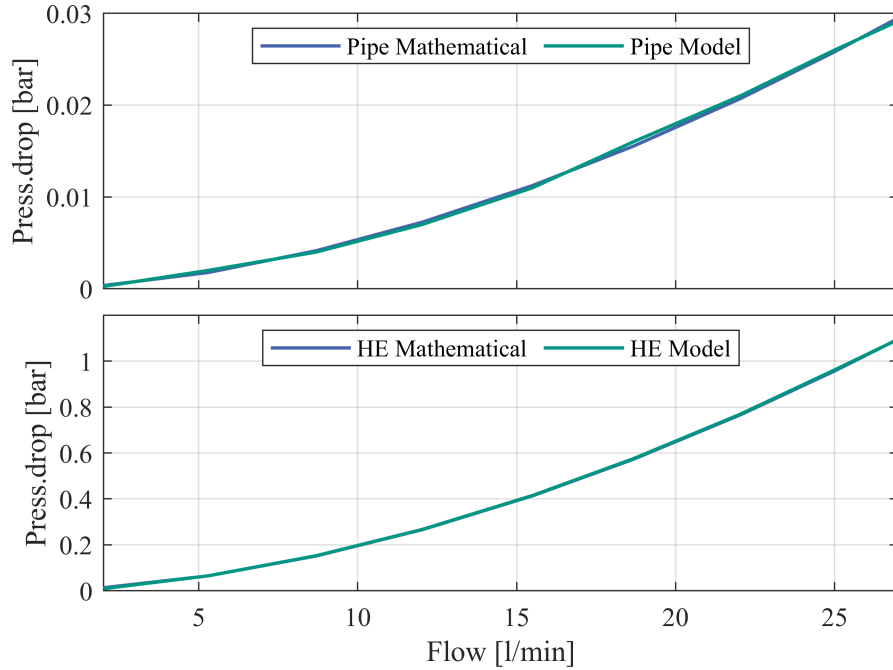


Figure 3.14: Maple vs Simscape mathematical and model comparison of the results

In the pipe system pressure drop there can be a little difference appreciated due to the values are really little and little deviations produce a big error. Nevertheless, the HE model appears to be identical and, actually, it is the important one, as the pipe system pressure losses are going to be neglected.

Another conclusion is the tendency of both curves. The tendency is parallel in both cases even if we have different parameterized models. In fact, both elements are modelled as an equivalent length pipe, therefore, it makes sense the tendency to be the same for different volumetric flows.

3.3 Laboratory Set-up

This chapter is based on the description of the full real laboratory set-up. Though this chapter, they are going to be described the different elements that form the laboratory set-up according to manufacturer data and to their characteristic charts. This is a key chapter inside this Thesis as not only has made a theoretical and modelling analysis as shown in the previous chapters, but it is going to be compared with the real behavior of the set-up. Furthermore, this is the reflex of the design of the set-up, showing that is not only paper based and that is actually built-up.

In this chapter, all the elements are going to be described, in a more or less deep way, in order to understand the behavior of the set-up. The idea is to describe the main function of each element in the set-up and their main characteristics. Every elements inside the set-up has a specific reason why it is part of this circuit and this is one of the objectives in this chapter: understanding the need of each element. In order to have an idea regarding the set-up, here we can see an overview of the full set-up.



Figure 3.15: Laboratory set-up overview of all the elements

Having clarified the main sense of this chapter, different elements are going to be listed below, shorted by primary to secondary elements.

3.3.1 Grundfos pump CRE 3-4 A-A-A-E-HQQE

Centrifugal vertical pump with opposite suction and discharge ports (inline design). The pump is equipped with a 1-phase, fan-cooled permanent magnet synchronous motor.



Figure 3.16: Grundfos CRE 3-4 A-A-A-E-HQQE PUMP [14]

For speed control, the motor has a frequency converter and PI controller housed in the motor's terminal box. The electronic speed control enables continuous adjustment of the motor speed and thus the pump output to the current demand. The set-point can be adjusted via a control panel on the motor terminal box. It can also be used to set the pump to "MIN", "MAX" or "Stop" operating modes. The Grundfos Eye status indicator shows the pump's operating status on the control panel as follows[14]:

- Switched on: Motor is running (green indicator lights illuminate and rotate) or Motor is ready for operation (green indicator lights illuminate continuously).
- Warning: motor is still running (yellow indicator lights are on and rotating) or has been switched off (yellow indicator lights are on continuously)
- Alarm: motor has been switched off (red signal lamps flash).

In the following table, there is a complete explanation of the characteristics of this pump given by the manufacturer.

Grundfos CRE 3-4 A-A-A-E-HQQE		
Technical data		
Characteristic	Value	Unit
Rated pump speed	3380	rpm
Rated flow	3.5	m ³ /h
Rated head	26.7	m
Maximum head	37.2	m
Liquid		
Characteristic	Value	Unit
Pumped liquid	Water	-
Liquid temperature range	-20..120	degC
Selected liquid temperature	20	degC
Density	998.2	kg/m ³
Electrical data		
Characteristic	Value	Unit
Motor type	71A	-
Rated power	0.55	kW
Power required by the pump	0.55	kW
Main frequency	50/60	Hz
Rated voltage	1x200-240	V
Rated current	3.45-2.90	A
Motor efficiency at full load	85.3	%

Table 3.17: Grundfos pump manufacturer technical data [14]

The pump is the heart of the set-up. It is vital to understand not only how it behaves, but how to control it. As a user, it is important to understand, first of all how to connect it to your device. Communication with the pump is possible via the Grundfos GO Remote app. There is a device called MI301 from Grundfos that is going to be used to control remotely the pump and connect your device to the pump. This device will permit selecting the characteristic curve we are going to work on. This means that if we set the pump in 70%, that is going to be the new virtual 100% of the pump. This means that when a 10V analog signal is introduced to control the pump, it will run in that 70% set point. Whenever the pump decreases it's power by decreasing the input voltage, it will reduce it proportionally until the minimum speed. This has an enormous advantage. Due to this virtual maximum set point, it is possible to achieve many OP. This virtual maximum will be controlled using the user panel.

It is possible to increase or decrease the maximum set-point by half a dot. By doing experimental research, this table could be really useful to understand not only the flow flowing through the pump, but the rotational speed as well.

Pump operation points for users			
Green point position	Flow [lpm]	Rotation speed [rpm]	% regarding the maximal operation point
1	7.58	854	32
1.5	8.98	908	34
2	10.34	967	36
2.5	11.74	1033	39
3	13.16	1104	42
3.5	14.57	1180	44
4	15.98	1262	47
4.5	17.41	1188	51
5	18.83	1443	54
5.5	20.23	1540	58
6	21.66	1644	62
6.5	23.04	1750	66
7	24.45	1864	70
7.5	25.84	1981	75
8	27.22	2102	79
8.5	28.66	2234	84
9	30.08	2370	89
9.5	31.50	2510	95
10	32.92	2657	100

Table 3.18: User information about Grundfos pump operation points

This table is going to be crucial to understand in every moment in which point we are working on. Actually, the incoming experiments are going to be based on the % of this table. Some conclusions could be done regarding this table. It is true that these experimental values could have been taken until 84% as the flow sensor does not allow to go further. However, it is easy to know the other values due to its linear tendency. If we go back to 3.7 and according to the characteristics of the manufacturer, the ideal 100% would be 3385rpm. According to this table, the maximal rotation speed is 2657rpm. This has 2 main reasons: The experimental values that the manufacturer gives are tested under different condition. We have to bare in mind that we have a certain set-up, with a resistance to the water (manufacturer tests the pump without resistance, giving the maximal possible value); additionally, we need to recall that the pump is taking pre-pressured water up to 2 bar, so again the conditions are different. Manufacturer information is a guide to know the actual limits of the pump. However, from this point on, we are going to work with table 3.17 that reflects the real working conditions.

3.3.2 Heat Exchanger Güntner, FLAT COMPACT GFHC

The heat exchanger has been manufactured by Güntner GmbH Co. The technical data has been provided by the manufacturer.

Güntner, FLAT COMPACT GFHC		
Fan Technical data		
Characteristic	Value	Unit
Fan type	VT03011U.1	-
Speed	1260	rpm
Current	2.2	A
Air temperature range	-30..50	degC
Technical data		
Characteristic	Value	Unit
Volume	6.9	l
Max. permissible pressure	10/0..0/-1	bar
Permissible min/max temperature	-50/+100..-50/+40	degC
Test pressure	11	bar
Test medium	compressed air	-
Electrical data		
Characteristic	Value	Unit
Main frequency	50/60	Hz
Rated voltage	1x100-240	V

Table 3.19: Güntner HE manufacturer technical data [9]

Data regarding the inside tube disposition is not available in the manufacturer data-sheet. This has been measured onsite, using the diameter and number of tubes and the total length of the HE.



Figure 3.17: Heat exchanger laboratory set-up

Güntner, FLAT COMPACT GFHC		
Tube technical data		
Characteristic	Value	Unit
Total length of Tube	90	m
Tube diameter	20	mm
HE longitudinal length	1	m

Table 3.20: Güntner HE tube data [9]

As user information, it is important to remember that a password is required to change HE settings. This password is 3795.

3.3.3 Electric Heaters Walser

In the set-up there are 2 Electric heaters which are going to be responsible for increasing the water temperature. These heaters had been manufactured by Walser Co and the technical data of each of them is the following.

Walser electric heater		
Heater technical data		
Characteristic	Value	Unit
Type	DLE	-
Max operation pressure	10	bar
Volume	0.014	m ³
Maximum temperature	112	degC
Electrical data		
Characteristic	Value	Unit
Main frequency	50/60	Hz
Rated voltage	3x400	V
Rated power	25	kW
Rated current	36	A

Table 3.21: Walser electric heater data [3]

It is necessary equipment to feed the electric heater. In this set-up an amplifier will be used to do so.



Figure 3.18: Electric Heaters laboratory set-up

3.3.4 Electric Amplifiers

The electric Amplifier is manufactured by Spitzenberger Spies. The three APS amplifiers are used for generating a three phase network system, either as a star connection with neutral or as a delta connection without neutral. Technical data has been taken from manufacturer data sheet.

Spitzenberger Spies DM/APS 45000 amplifier		
Amplifier technical data		
Characteristic	Value	Unit
Type	DM 45000/APS	-
Main frequency	50/60	Hz
Power AC	45000	VA
Power DC	45000	W
Short time Power AC	90000	VA
Peak current	616	Ap
Peak current parallel mode	1848	Ap
Voltage	230/400	V
Current	3x65	A

Table 3.22: Spitzenberger Spies amplifier data [22]



Figure 3.19: Spitzenberger amplifier laboratory set-up

3.3.5 Electric Valve

The electric valve is going to be used as an auxiliary element to the pump in order to control the flow. In fact, this element is going to be crucial in order to work below the minimum operation point of the pump.



Figure 3.20: IMI Hydronic TA-Slider 160 electric valve[7]

This electric valve has been manufactured by IMI Hydronic Engineering and has the following characteristics.

TA-Slider 160 IMI Hydronic electric valve		
Electrical valve technical data		
Characteristic	Value	Unit
Type	TA-Slider 160	-
Main frequency	50/60	Hz
Power supply	24	VAC/VDC
Power consumption operating	0.6	W
Power consumption operating	0.25	W
Input signal	0(2)-10	VDC
Output signal	0(2)-10	VDC
Actuating speed	10	s/mm
Stroke	6.9	mm
Actuating force	160/200	N

Table 3.23: TA Slider 160 IMI Hydronic electric valve data [7]

3.3.6 Pressure Diaphragm Vessel

This device will be the responsible for keeping the pump inlet water pre-pressurized. It's working principle is based on an inside non-rigid nitrogen gas vessel. This gas is pressurized as well as permits water in, by keeping in a certain pressure without any external work. This diaphragm pressure expansion vessel has been manufactured by Reflex.



Figure 3.21: Reflex N25 pressure diaphragm vessel [18]

Characteristics of this pressure diaphragm vessel are the following.

Reflex N25 pressure diaphragm vessel		
Pressure diaphragm vessel technical data		
Characteristic	Value	Unit
Type	N25	-
Nominal volume	25	l
Usable volume max	24	VAC/VDC
Permissible flow T supply	3	degC
Permissible operating overpressure	3	bar
Gas inlet pressure from factoryl	1.5	bar
Gas	N2	-

Table 3.24: Reflex N25 pressure diaphragm vessel data [18]

3.3.7 Pressure, temperature and flow transmitters

For collecting the required data 3 types of transmitters have been used. The data from manufacturer's data sheet is collected in the following tables for each of the sensors.

IFM PT0505 pressure transmitter		
Pressure transmitter technical data		
Characteristic	Value	Unit
Type	PT0505	-
Measuring range	0..4	bar
I/O signal	analog	-
Analog current output	4..20	mA
Step response time	4	ms
Uncertainty		
Repeatability	+/-0.1	% of the span
Characteristics deviation	+/-1	% of the span

Table 3.25: IFM PT0505 pressure transmitter data [11]



Figure 3.22: IFM PT0505 pressure transmitter [11]

IFM TA3317 temperature transmitter		
Temperature transmitter technical data		
Characteristic	Value	Unit
Type	TA3317	-
Measuring range	0..100	degC
I/O signal	analog	-
Analog current output	4..20	mA
Resolution	0.04	degC
Uncertainty		
Precision analog output	+/-0.3	% of the span
Temperature coefficient	+/-0.1	% of the span

Table 3.26: IFM TA3317 temperature transmitter data[12]



Figure 3.23: IFM TA3317 temperature transmitter [12]

IFM SM6000 flow transmitter		
Flow transmitter technical data		
Characteristic	Value	Unit
Type	SM6000	-
Measuring range	0.1..25	l/min
Display range	-30..30	l/min
I/O signal	analog	-
Analog current output	4..20	mA
Resolution	0.02	l/min
Uncertainty		
Accuracy	+/-0.8	% of the measuring range
Repeatability	+/-0.2	% of the measuring range

Table 3.27: IFM 6000 flow transmitter data [10]



Figure 3.24: IFM SM6000 flow transmitter [10]

3.4 Experimental Results Analysis

Across this sections a wide and detailed description of the results obtained using the laboratory set-up will be described, as well as a comparison between the already commented models.

3.4.1 Measurement and Uncertainty

Each measurement is subject to uncertainties. For the evaluation of the measurement results uncertainties are determined in this work using the method according to "GUM" (Guide to the Expression of Uncertainty in Measurement)[13]. With this method, a certain range of variability with "possible values" is allowed. The aim of the measurement uncertainty analysis is to quantify this variability and express it in a numerical value.

Measurement uncertainty analysis comprises two procedures. These procedures are called "Type A and "Type B". The "Type A" procedure describes the uncertainty on the basis of the actual actual measured values in connection with the number of measurements. With the procedure "Type B", the uncertainty of measurement of the sensor technology or by manufacturer's data or calibration certificates.

In this report, the type B method is going to be used. Different sensors from the set-up have been tested under certain conditions obtaining a detailed calibration certificate. Therefore, we are going to make use of these certificates to evaluate the uncertainty.

In the following table, there are some characteristics of the calibrated sensors.

Overview of sensor measuring range and uncertainty			
Sensor	Lower measuring range	Upper measuring range	Uncertainty Type B
Water flow rate	0.2l/min	30l/min	±0.4 l/min
Temperature HE input	0°C	100°C	±0.45°C
Temperature HE output	0°C	100°C	±0.45°C
Pressure HE input	0 bar	4 bar	±0.0021 bar
Pressure HE output	0 bar	4 bar	±0.0021 bar
Pressure pump input	0 bar	4 bar	±0.0021 bar
Pressure pump output	0 bar	4 bar	±0.0021 bar

Table 3.28: Overview of sensor lower and upper measuring range and uncertainty [11][10][12]

In the case of indirect measured quantities such as electrical and thermal power, the error propagation is taken into account. The error propagation describes the interaction between several of several measurement uncertainties. The error propagation affects directly the thermal power, being its expression.

$$P_{th} = c_{KW} \cdot \rho_{KW} \cdot \dot{V}_{KW} \cdot (T_V - T_R) \quad (3.27)$$

For this equation, the derivation of the uncertainty is expressed as it follows.

$$u_{P,th} = \sqrt{\left(\frac{\partial}{\partial \dot{V}_{KW}} P_t h^2\right) \cdot u_{\dot{V},KW}^2 + \left(\frac{\partial}{\partial T_V} P_t h^2\right) \cdot u_{T,V}^2 + \left(\frac{\partial}{\partial T_R} P_t h^2\right) \cdot u_{T,R}^2} \quad (3.28)$$

$$u_{P,th} = \sqrt{c_{KW}^2 \cdot \rho_{KW}^2 \cdot \left((T_R - T_V)^2 \cdot u_{\dot{V},KW}^2 + \dot{V}_{KW}^2 \cdot (u_{T,R}^2 - u_{T,V}^2)\right)} \quad (3.29)$$

For the numerical determination of the uncertainty, the manufacturer data is used in combination with equation 3.29. The result of this equation will give us the result of minimum and maximum values of thermal power according to the uncertainty calculated.

Thermal power max/min values	
Control of thermal emulator	Thermal power
Minimal 30%	10kW \pm 275W
Maximal 100%	15.6kW \pm 474W

Table 3.29: Maximum and minimum values of thermal power of the thermal emulator according to uncertainty range

3.4.2 Model Validation

After having developed and studied the thermal emulator Mathematical and Simscape models, defining its behavior and parameters, it has been validated with experimental results. To perform this task 2 types of experiments have been done. The main goal is of course comparing and contrasting the experimental results with the model ones. Nevertheless, the idea is also making use of 2 flow controlling tools: the pump and the electric valve. Therefore, not only will we obtain experimental results regarding HE pressure drop for different flows, but also the real behavior of the pump and the valve.

In order to obtain these type of results, a first experiment has been done to compare pump and valve controlling behavior regarding HE pressure drop for different flows. Tests regarding pump control have been driven for different rotational speed of the pump and a variation of the pump input electric signal to reach different flows. In the case of the valve controlled system, however, pump rotational speed has been kept during the experiment and the valve signal has been varied in this case, varying slowly. This table shows a comparison between the 70% test results for pump and valve control.

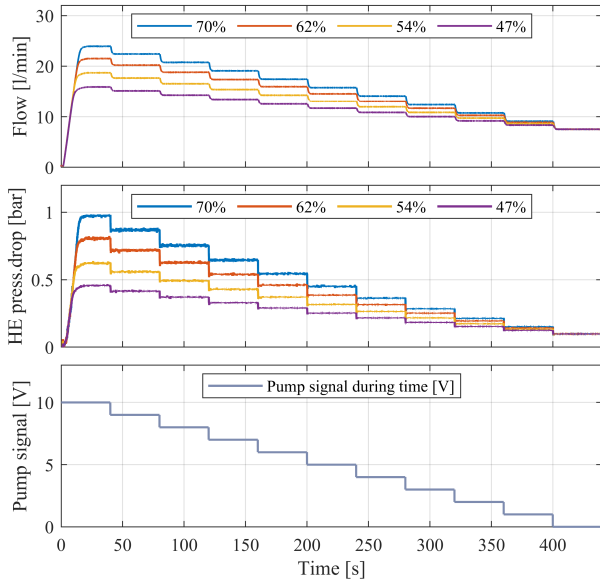


Figure 3.25: Pump controlled HE pressure drop during time for different flows, due to a change in the pump input electric signal

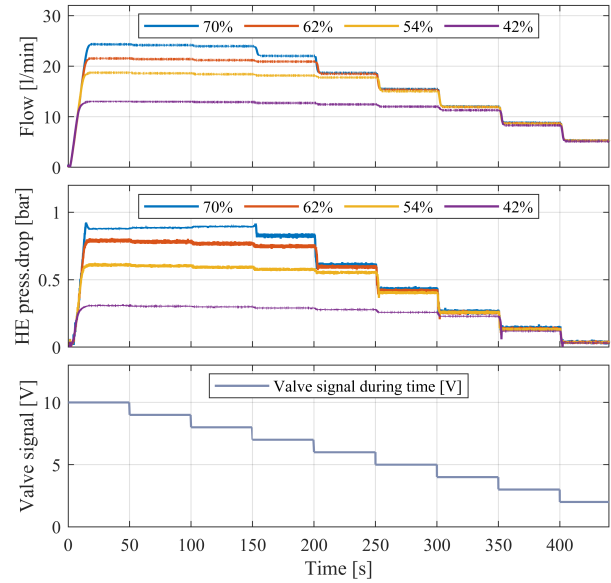


Figure 3.26: Valve controlled HE pressure drop during time for different flows, due to a change in the valve input signal with pump signal constant

The percentages that appear in the legend make reference to the achievable rotation speed of the pump, in this case 2657 rpm according to table 3.17. According to the results shown in both table, we realise that a linear change in the input signal of both devices brings a linear pressure drop on the HE.

This fact is much more appreciable in the pump controlled case. However, for the valve signal, we realise that the effect of the valve is barely noticed until the valve signal reaches one point, where the behavior of the flow and the HE pressure drop equal the pump controlled chart. This is because the valve makes no effect until the valve closing % matches the flow capacity of the pump.

In both cases, therefore, we conclude the linearity of both controlling systems. It seems that the pump controlling way is more accurate than the valve one and, for this reasons, it is advisable to make an exhaust control of it using the pump. Furthermore, a really interesting conclusion we can see from the pump test is that depending on the initial set-point of the valve as maximal speed, the input decreasing signal divides in equal rotating speeds (10 divisions in this case) of the pump, allowing to have a wide variety of different flow vs HE pressure drop relation. This is an advantage if we want a really specific point of the pump.

As a disadvantage, we can see that the pump working in its minimum rotational speed, can achieve a minimum flow of 7.5 l/min. The only possibility to go below this point is by making use of the electric valve. In the next figure we can see a plot where the pump is working near the minimum point and controlled by the valve.

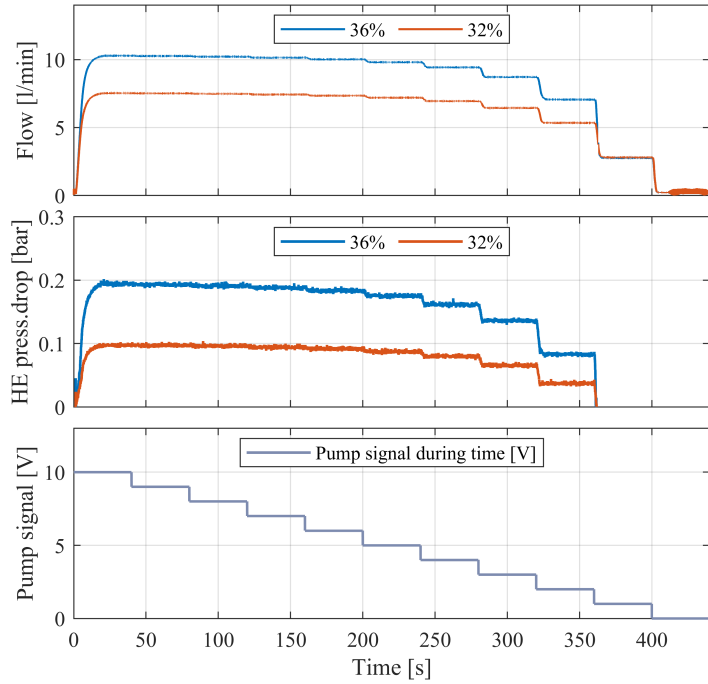


Figure 3.27: Valve controlled HE pressure drop for low pump rotating speed

According to this graphic we conclude that using the electric valve is possible to go below the minimum flow of the pump. We appreciate a instability during the time with practically no cut-off of the flow. Furthermore, from 3V to 0V it is clear that the valve starts to change the flow. However, this change happens in a non-linear way. This is another disadvantage of the valve.

This data is really useful to compare the correlation between the flow and the HE pressure drop in a unique graph. Using the numerical data obtained from the previous figures, we obtain a correlation between these two variables in both cases, for valve and pump controlled tests.

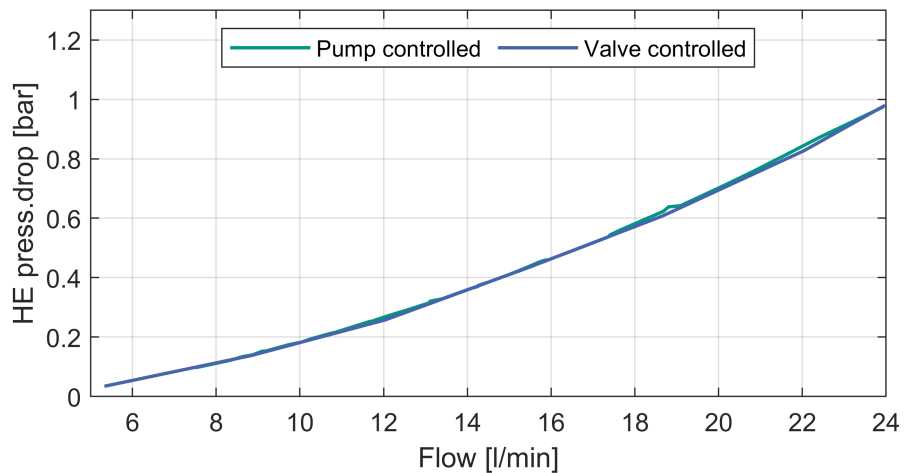


Figure 3.28: Correlation between flow and HE pressure drop for pump and valve controlled cases

In figure 3.28 we analyse a specific working range for pump and valve. We cannot actually say that out of this range the behaviour is going to be this way. The very first conclusion that we obtain from this figure is that the correlation is not linear, it has a polynomial behavior instead. Furthermore, we can see that both curves practically match. For this reason, another important conclusion to be made is that this relation does not depend on the way of controlling the flow; pressure drop in the HE is only dependable on the flow, no matter how this is controlled. This is an important feature to take into consideration.

Once we have studied both experimental behaviors, it is important to compare them with the model. As both models, mathematical and simulation, practically match, the Matlab Simscape model has been chosen to avoid too many curves. The result of this comparison could be seen in the following figure.

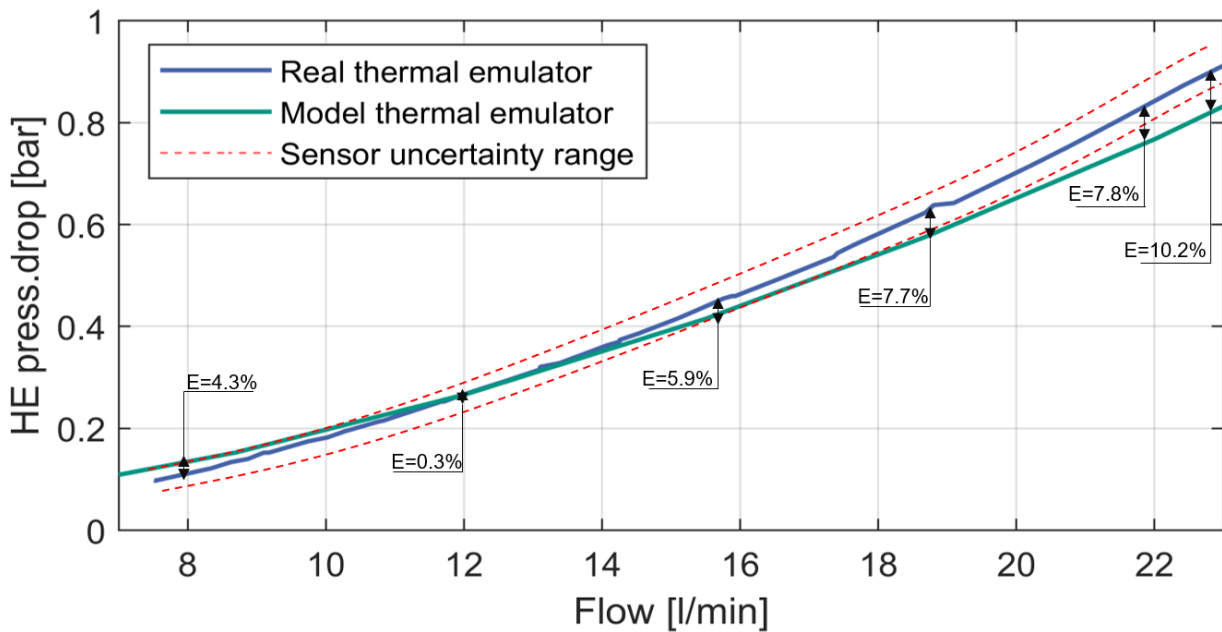


Figure 3.29: Model and experimental results comparison regarding the flow and HE pressure drop

We can appreciate that the model and the experimental results match in a high extent. There could some dispersion appreciated for for high flows. In the next table, the error of both, model and experimental will be analyzed.

Comparison Model and Experimental results and Error				
Model		Experimental		Deviation
Flow [l/min]	HE ΔP [bar]	Flow [l/min]	HE ΔP [bar]	Error [%]
7.98	0.153	8.7	0.135	11.7
12.03	0.267	12.03	0.266	0.3
15.5	0.415	15.5	0.441	5.9
18.67	0.575	18.67	0.623	7.7
21.89	0.769	22.03	0.831	7.8
23.97	0.899	23.97	0.94	10.21

Table 3.30: Comparison model and experimental results and error

According to the results we can see an error in some points for very high and low speed rotations. We need to bare in mind that the uncertainty of the pressure sensors is of 0.021bar. We can appreciate this uncertainty band in 3.30 and we can conclude that in some points the errors could be minimized. We do not really now due to the uncertainty. Nevertheless, if we see the numerical values, we realize that the difference between them is not that important and we could conclude that the model is accurate to the experimental results.

3.4.3 Maximum Rate of Change

This chapter will deal with the thermal field instead of fluid mechanic field. The objective of this chapter is to explain how fast/slow is going to be reached the heat exchange between the two working mediums: water and air. The analysis will be done regarding the water inside our set-up. If we remember the equation 3.2:

$$q = \dot{q}_j = \dot{m}_j \Delta h_j = (\dot{m} c_p)_j \Delta T_j \quad (3.30)$$

We can conclude that the heat exchange is going to dependant on \dot{m} and on ΔT of the flowing water. For this reason, the aim of this chapter is studying both, the temperature difference water suffers and the effect of different flows. For doing so, we are going to study in separate ways the rate of change regarding the flow and regarding the thermal power.

To begin it is important to be aware of the difference between controlling the flow using the valve or the pump. We have already seen that there is no difference in terms of flow and HE pressure drop correlation. However, it is important how it is this behavior in real time simulation. The way of doing so is again utilizing both, valve and pump control to see the difference regarding the time it takes to reach the steady state. Here we can see both experimental results regarding pump and valve controlled simulations, respectively.

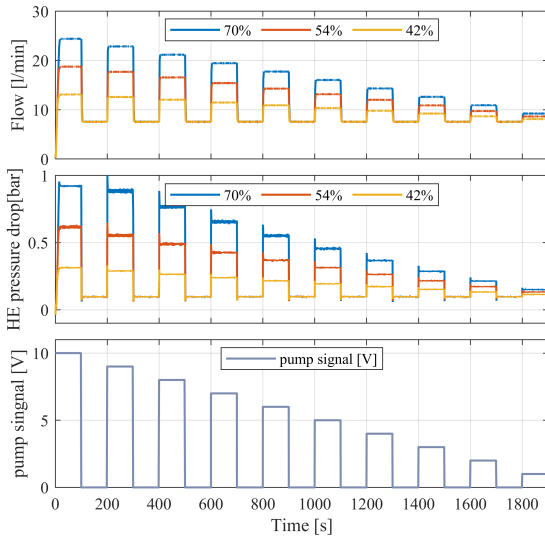


Figure 3.30: Pump controlled flow rate of change

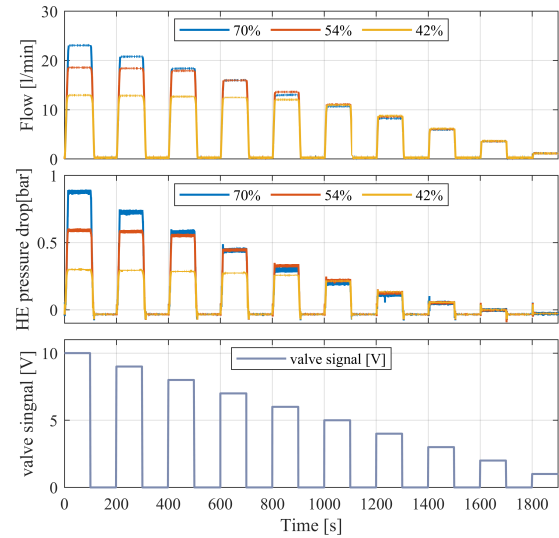


Figure 3.31: Valve controlled flow rate of change

They both seem actually really similar to each other. In both cases we can appreciate the symmetry, being clear that they take the same time no matter if they are increasing or decreasing the flow through the device. Furthermore, there are some key differences that we can conclude. First of all, we see that in the pump case the results are much more distinguishable, while in the valve case there is sometimes a non-sens mix regarding the steady state. Nevertheless, we have again the problem with the pump flow limitations, where we would need to use obligatorily the valve. To finish with, it will be interesting to know how much time does the operation of valve open/closing take and same for the pump.

To do so, another more clarifying figure will be presented as it follows.

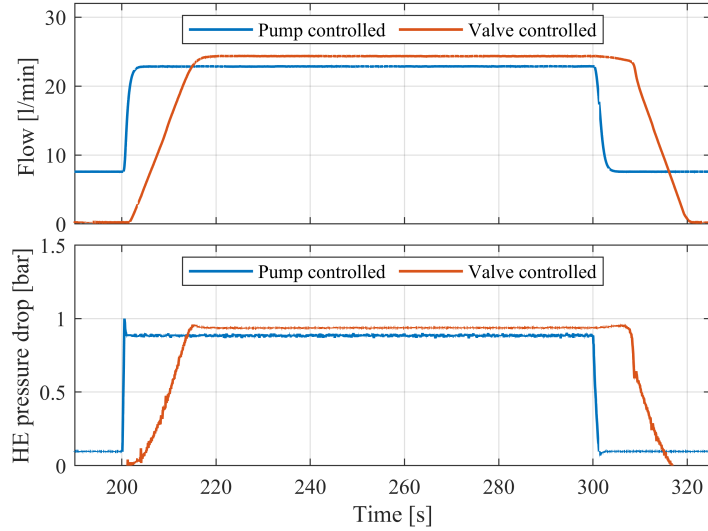


Figure 3.32: Detail of rate of change pump and valve controlled

In 3.32 we can clearly appreciate the time it takes to open or close the flow. In the case of the pump, this takes less than 3 seconds in both ways while speeding up and while slowing down. In the case of the valve, we see that it is non-symmetric. The slope on the opening and closing is not equal, having a change rate of 17s/V and 13 s/V respectively. This happens because the force the water does into the valve makes it easier to close the valve and it hampers the opening instead. If the idea is to make fast flow changes, the valve is not a good tool to be used. Actually, the valve will be used only in case we want to target a really reduced flow. An interesting question would be to use a much faster valve. However, the expected result could be the water hammer effect. This pressure wave can cause major problems, from noise and vibration to pipe rupture or collapse.

Once having decided that pump is going to be the tool used to control the flow, now another test will be done using the flow variation method. It is important to remember the correlation between the mass flow and the thermal power.

$$P_{th} = \dot{m} \cdot c_p \cdot \Delta T \quad (3.31)$$

In this case the objective will be evaluating the rate of change regarding the time it takes the thermal power to reach the steady state and how the thermal power varies with a flow variation. To do so, we will use a constant electrical power supply and a variable to see in each stage how much time it takes to reach the steady state. In this figure, we can see a detailed plot of the commented experiment.

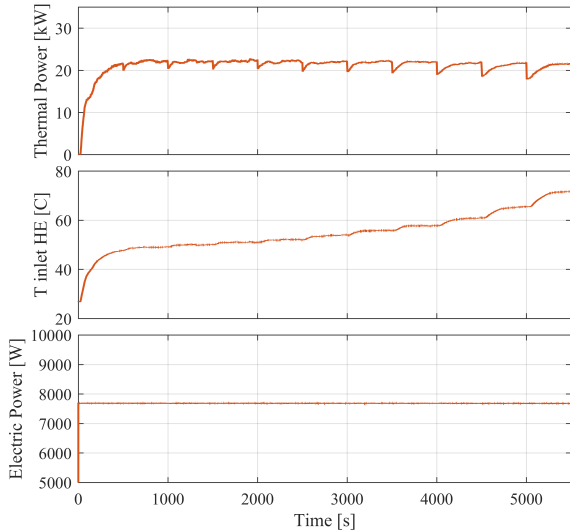


Figure 3.33: Flow variable and electric power constant thermal power rate of change analysis A

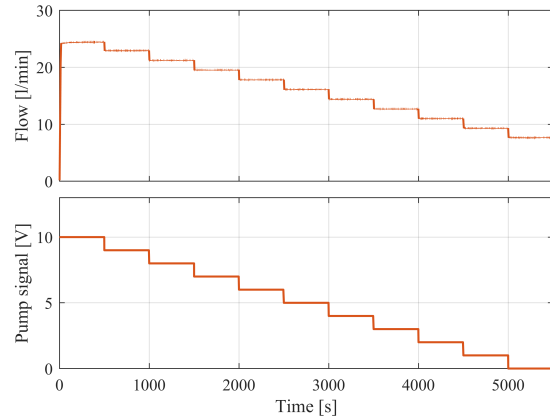


Figure 3.34: Flow variable and electric power constant thermal power rate of change analysis B

In the above figure we see how at a constant electric power and making a variation of the water flow, the thermal power is barely affected. We should try instead with the electric power, as the flow is not enough to cause a noticeable thermal power. The rate of change, however is important, as it refers to the transient behaviour of the thermal emulator. The objective of this stage is to be as short as possible. The experiment consists of 500 seconds margin for each of the pump input electric signal in order to reach the steady state. There are some differences in the rate of change of thermal power regarding different flows. In the next figure, we can see a detailed plot of two different states, in order to analyse the transient state.

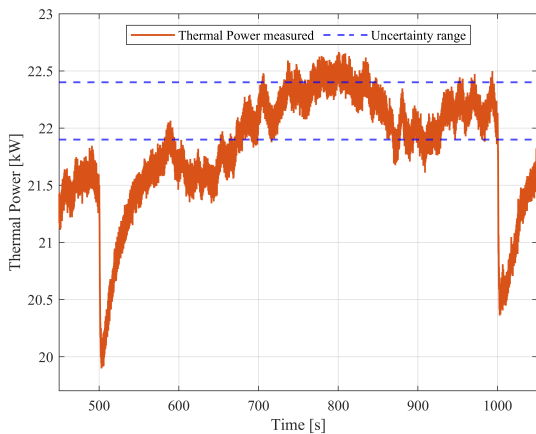


Figure 3.35: Flow variable and electric power constant thermal power rate of change analysis detail A for 9V pump signal

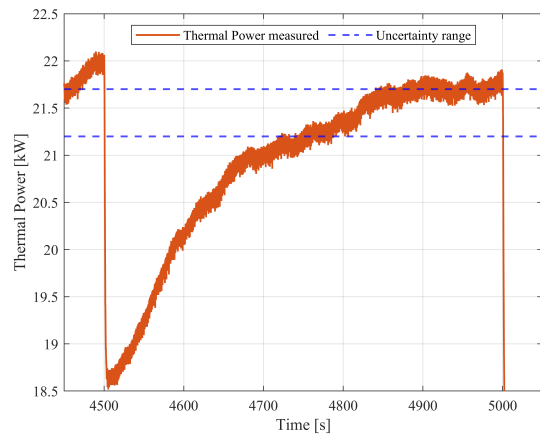


Figure 3.36: Flow variable and electric power constant thermal power rate of change analysis detail B for 2V pump signal

The rate of change will be defined as the time it takes to reach the steady state from a

thermal power specific point to the final state. In the case of 9V pump signal, we can see that for a 2kW change it takes 100 seconds, while in the case of 2V for a change of 2.5kW up to the steady state takes 200 seconds. Therefore, we have 20W/s and 12.5kW/s for 9 and 2V cases, respectively. We can conclude in this case that while the flow decreases, the rate of change decreases as well. This last affirmation makes sense as if we take a look into 3.2, the heat exchange is proportional to the flow, therefore the maximum rate of change will come with the maximum flow as showed in this experiment. Therefore, it is important to work with higher flows to shorten the transient stage.

Once clarified the flow change part, now it is the turn to evaluate the other way round. Instead of focusing on the flow effect, now the idea is to maintain constant the flow and change the electric power during the time. The relation between the electric power and the thermal power is the following.

$$P_{th} = 3 \cdot P_e \quad (3.32)$$

In the following experiment, we expect therefore to have significant changes in the thermal power according to 3.32. The results obtained are the following.

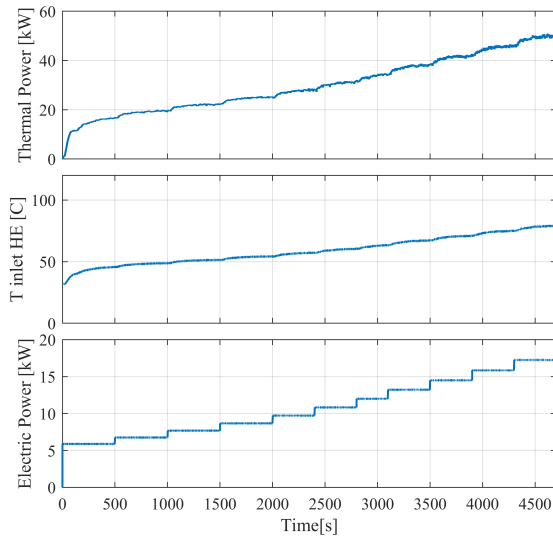


Figure 3.37: Electric power variable and flow constant thermal power rate of change analysis A

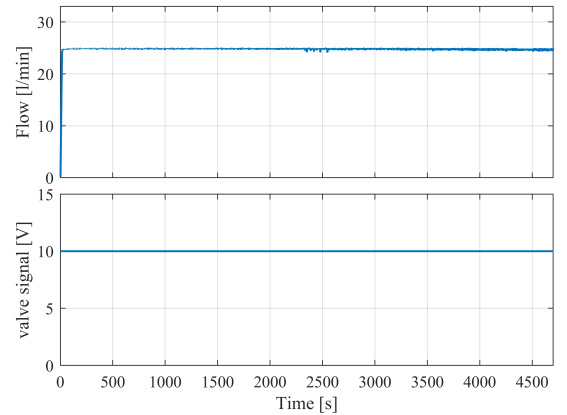


Figure 3.38: Electric power variable and flow constant thermal power rate of change analysis B

In this case, this experiment has been done 10 times, each of them with a different valve signal from 10 to 1. In this case it was not that important the rate of change or how fast we could achieve the steady state. Instead, we wanted to have a full range of flow-electric power operation points in order to see the limits the set up had. The valve is useful in this case because it permits us going below 7.5l/min. The results of these 10 different experiments are summarized in the following table, having temperature values in degC.

Temperature [°C] different scenarios for different flow and electric power combinations											
Voltage[V]	Power[W]	Flow for different valve position [l/min]									
		1.09	5.3	8.7	12.03	15.5	18.7	22.03	23.9	24.1	24.33
150	5890	69.3	66.27	58.64	44.24	43.64	40.41	43.01	40.81	36.68	45.41
160	6748	77.16	81.5	69.73	53.21	46.89	42.22	46.23	44.15	41.90	48.69
170	7682	+90	+90	77.32	57.14	50.75	44.48	49.21	46.79	44.88	51.28
180	8673	+90	+90	84.95	61.18	54.26	48.17	51.95	49.90	47.57	54.18
190	9726	+90	+90	+90	65.51	57.99	51.44	54.78	52.67	50.50	57.08
200	10833	+90	+90	+90	69.86	61.67	54.57	57.95	55.97	53.76	60.31
210	11994	+90	+90	+90	74.72	65.73	58.61	61.22	58.86	57.05	63.36
220	13215	+90	+90	+90	80.01	69.58	62.66	64.84	62.6	60.60	67.08
230	14490	+90	+90	+90	89.39	73.74	66.18	68.33	66.14	64.03	70.68
240	15856	+90	+90	+90	89.35	77.42	67.94	72.32	70.11	67.98	74.56

Table 3.31: Temperatures in °C for different combinations of flow and electric power supply

This table shows the different combinations of electric power and flow and the resulting temperature on the steady state. Table 3.31 allows us to know exactly where to work in safety conditions. It should be clear that this is experimental and it could happen that depending on the starting conditions, in a really hot day, these results could vary. However, it is a table to have an idea on which ranges we could not work under no circumstances. The electric heaters have a safety system that when it gets 90°C, the amplifiers go off as a security measure. Of course it is advisable not to go into these thresholds and work in safety conditions.

Furthermore, it is interesting to study the rate of change regarding the thermal power with the electric power application. For this purpose, the following detail of 3.37 is showed.

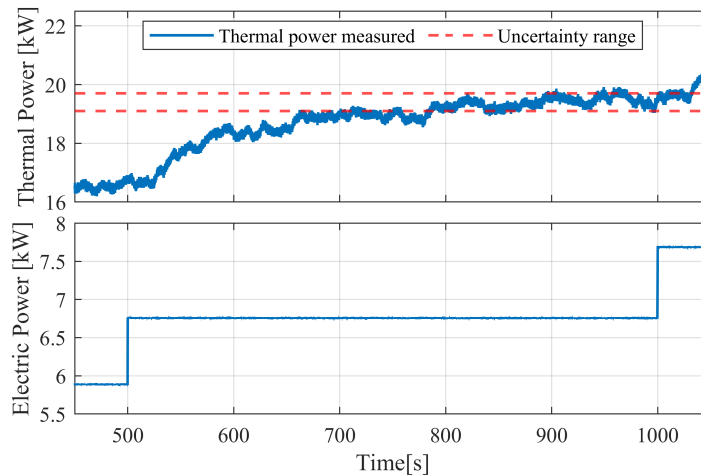


Figure 3.39: Detail of electric power variable and flow constant thermal power rate of change analysis to evaluate thermal power rate of change

Considering 3.32, we obtain a rate of change of 600W/s. Therefore, we are going to achieve thermal power set-point using electric power.

3.4.4 Limits of Applicability

There are several limits with different origins that do not allow to work in every conditions and they will be described through this chapter.

First of all, the feature of trespassing 90°C is a threshold that cannot be trespassed. This is for security and of course not to have a change in the state of water, as a gaseous state of water could damage irreversibly the pump, for example. A experiment has been done in order to test that this 90°C threshold is not trespassed.

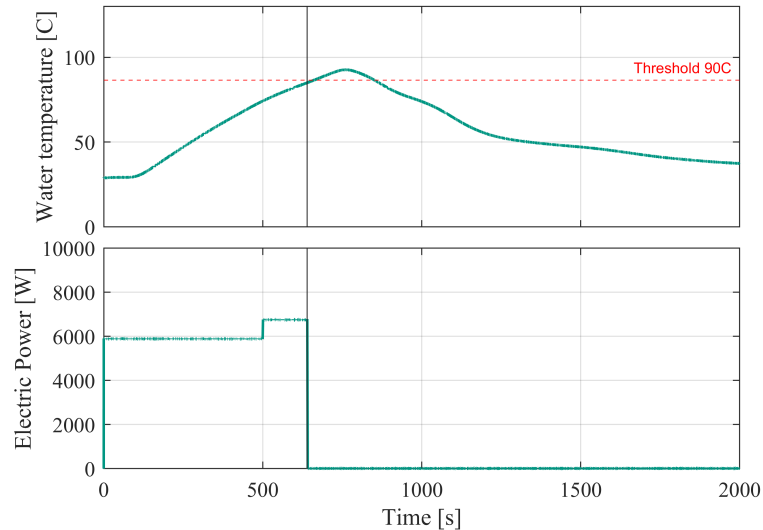


Figure 3.40: Amplifier security switch off above 90°C

In this figure we can see how the electric power switches off when the temperature signal is 90°C . As we can see in 3.40 after the switch off the temperature continues rising even if the amplifier does not feed the heaters. This is due to there is still a remaining heat flux that leads the temperature to continue increasing during some time. However, once this increase stops, the temperature falls rapidly.

Another limit of application is regarding the mass flow sensor. We are not able to perform the full power of the pump as we are not able to read that value. Therefore, it would be advisable to have a greater range mass flow sensor to be able to work in a wider range of flows. Furthermore, in this direction of flow, below the minimum operation point of the pump, valve should be used to regulate the flow. The disadvantage is that the valve deals with big flow jumps and we are not able to really adjust the point of operation to the one we really need.

Time taken to get to the steady state is also a limitation regarding the thermal behavior. It is a minimum of time to get to the steady state and if any flow change should be done before reaching that point, no valid result will be obtained.

Chapter 4

Real modelling on virtual household

4.1 RTDS real time simulator and MGT behavior target

This chapter will enable a comparison between the thermal emulator and the existing MGT of the household. We need to bare in mind that the objective is to achieve an equal behavior of the thermal emulator so as to work in parallel with the MGT.

This comparison will be made with a real time simulator, used at the same time to make every experimental tests. This real time simulator has been manufactured by RTDS Technologies and it is called NovaCor RTDS Simulator[26].

This RTDS Simulator has allowed utilities, manufacturers and research institutions to test multiple devices in a closed loop with the simulated network while easily adjusting network parameters, contingency scenarios and device setting for the first time.

Inside the NovaCor there is a custom-built board unit featuring IBM's POWER8 processor. 10 powerful cores run at the same time at 3.5GHz. This multi-core system process makes NovaCor capable of more faster and complex real time simulation. The configuration permits the simulation to run directly on the processor for unparalleled speed and efficiency.

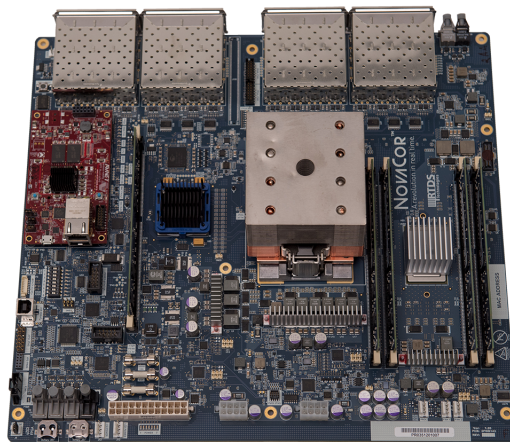


Figure 4.1: NovaCor RTDS custom-built board unit [26]

There is a RTDS Simulator software that could be configured on the user's PC, called RSCAD FX. This software allows the configuration, execution and analysis of real-time simulations. This RSCAD FX has different available modules and capabilities.

- Circuit construction: There is the possibility of defining single- or three-phase circuits. There is a extensive component library to easy create the required circuit.
- Operator's module: Start, stop and possibility to interact with the simulation in real-time. The user can adjust parameters, visualize errors and view real-time simulation data.
- Component builder: Using C language and a drawing facility to create user-defined power system or control components that run in a real time environment with the help of existing library components.
- Manual and documentation: Comprehensive documentation available for every user regarding library components, software modules, sample cases and tutorials.

The connection among the user PC device, NovaCor RTDS and the device under test is relatively easy. There are 2 types of connection that connect NovaCor RTDS with user PC workstation and test device. PC and real time simulator using a simple Ethernet link, while the device under test needs 2 auxiliary cards to successfully connect to the simulator.

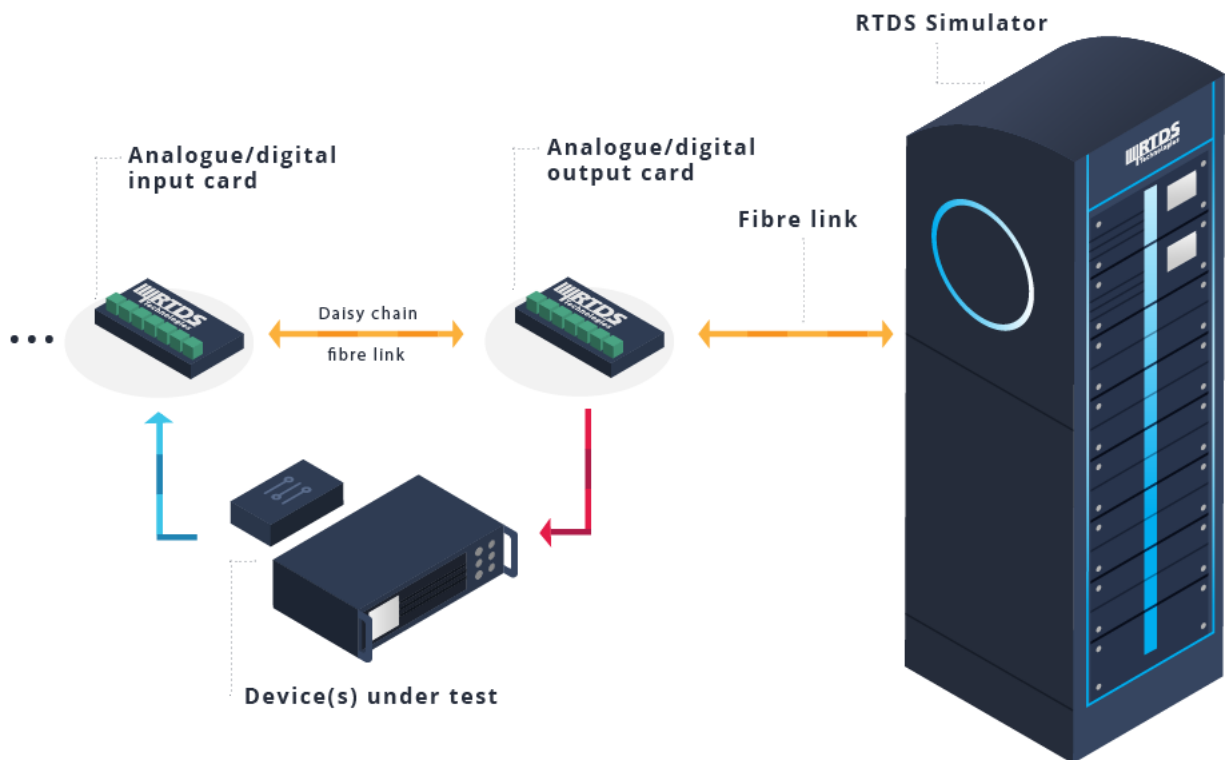


Figure 4.2: NovaCor RTDS connection to device under test[26]

These cards are the I/O (input and output) and are used to connect external devices to fibre-optic ports on the rear of a NovaCor unit. These cards are called GTA0 and GTA1 analogue cards and connect the external equipment at ± 10 V_{peak} to the simulator. They

are both installed in the test device and it receives the analog signal from the different sensors that are going to be the input signal for the real-time simulator. They are both quite similar, see, as an example, the GTAI card image.

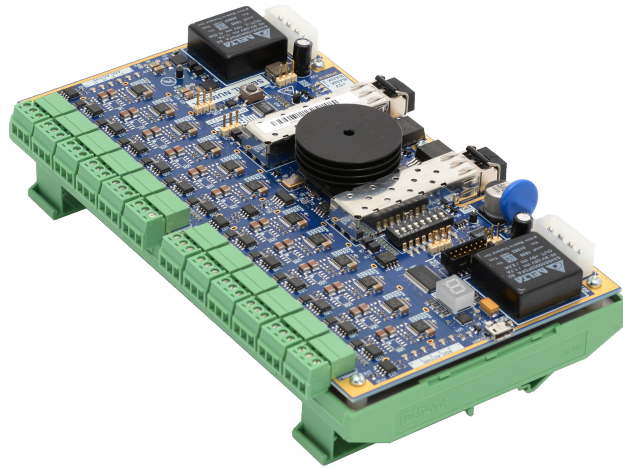


Figure 4.3: GTAI analogue card[26]

This NovaCor real-time simulator is going to be the heart that will permit us compare the thermal emulator with the MGT. To emulate the MGT behavior we have available data taken from the real set-up of the MGT. The idea is to reproduce this behavior with the thermal emulator real set-up and make a comparison between both devices. This is the target behavior of the MGT that is going to be reproduced.

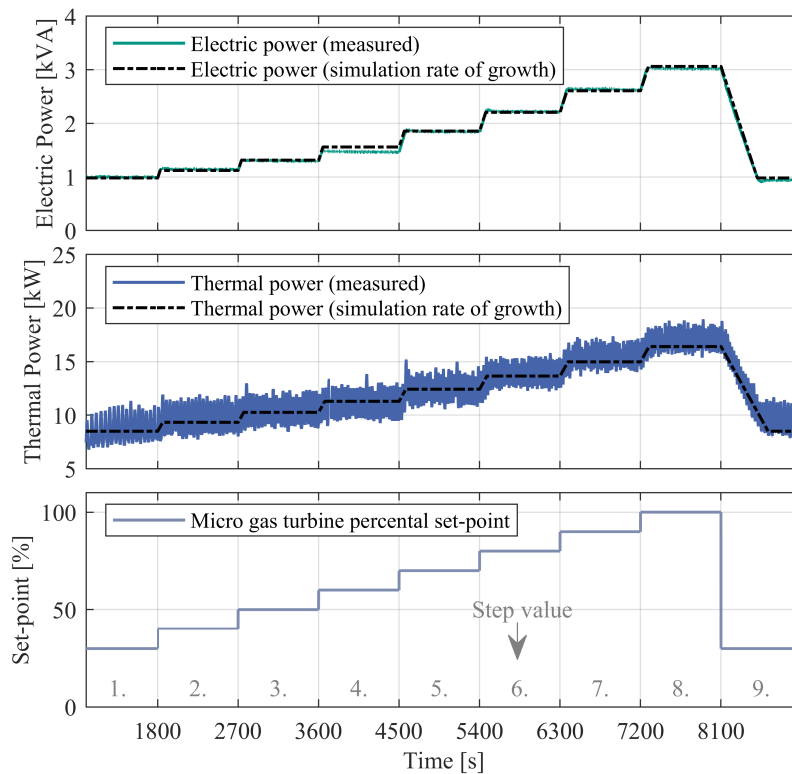


Figure 4.4: MGT real device behavior and target

The goal is to reproduce the thermal power the MGT produces with the thermal emulator. Furthermore, we have to take into consideration that the output temperature in the MGT is 55degC, therefore, we have to reproduce that temperature as well. We need to take into consideration again that the variables that take part in the heat exchange are the flow and the temperature difference, so we need to put the focus on these 2 variables. For doing so, 2 types of PI controllers will be installed in order to obtain the target result.

4.2 Electric variable power PI controller to control thermal power

This first PI controller has the objective of controlling the target thermal power from MGT data. This experiment will be run using an electric power variable input while the flow remains constant. After several simulations, here we can see a comparison for different P and I couple values.

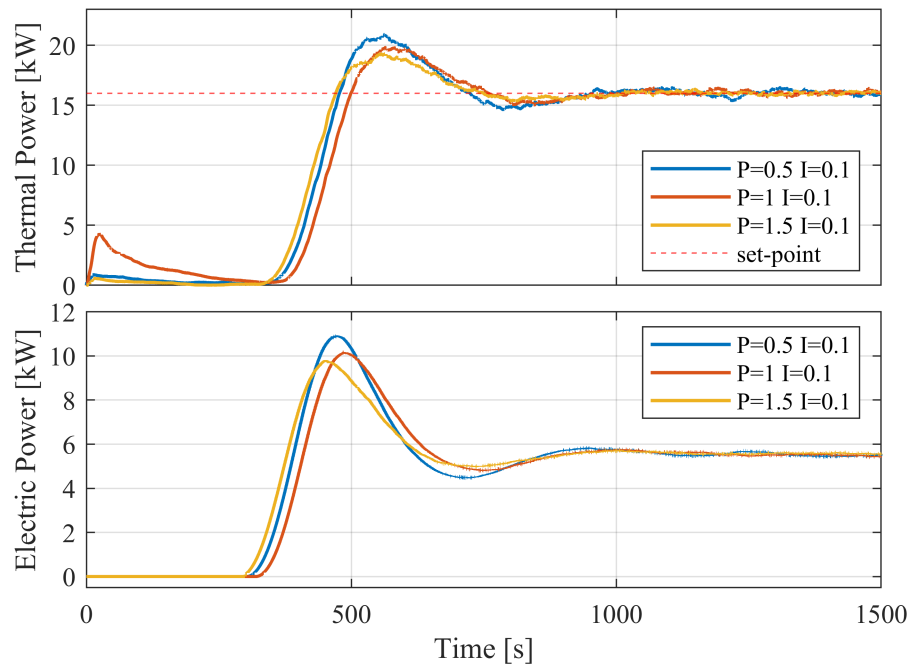


Figure 4.5: PI controller for thermal power using a variable electric power

In this PI controller we can see how the set-point is reached in all cases. However, due to the shape of the figure, the best case would be P=1.5 and I=0.1 case, as the set-point is more rapidly as the others achieved. The oscillations around the set-point are not that notorious as in the other cases, therefore, this is the parameterization of PI we are going to use. The idea, in the future, is to implement in parallel another PI in order to control the output temperature of the HE. This PI will influence the pump and, therefore, the flow. For this research, however, this PI is out of scope and it is not going to be installed.

4.3 MGT and thermal emulator comparison and discussion

This chapter will describe the final target of the thermal emulator: Emulating the behavior of the MGT. Actually, it is not going to be possible to emulate the transient behaviour of the MGT. Instead, this controller will focus on the set-point and indeed, on the steady state of the MGT.

After doing some experiments on this topic, finally we have been able to find out a result and the respective target comparison between the thermal emulator and MGT.

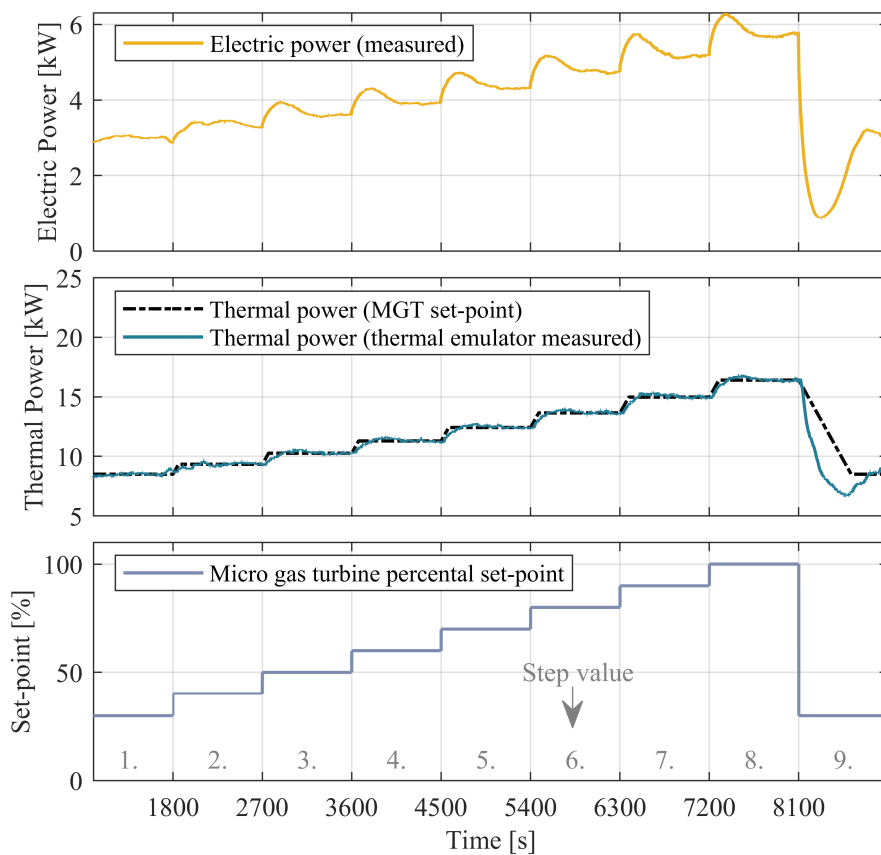


Figure 4.6: Comparison between Micro Gas Turbine and Thermal Emulator thermal power output and transient behaviour

The immediate conclusion we make from this result is that the steady state is reached and that the device emulates more or less accurately the set-point of the MGT. This set-point is reached thanks to the electric power which is the responsible for increasing the thermal power in the thermal emulator. However, there is a transient behavior component that is controlled by the flow across the HE. In order to analyze this transient behavior in a more accurate way, a detail of this comparison is showed.

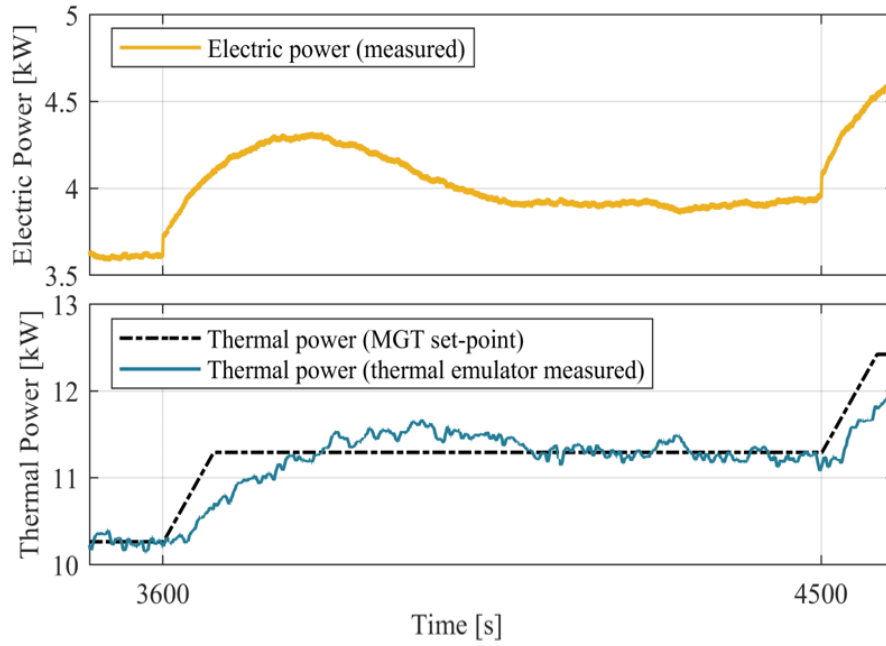


Figure 4.7: Detail of the comparison between Micro Gas Turbine and Thermal Emulator thermal power output to analyze the transient behaviour

We can analyse figure 4.7 within 2 phases. The first phase, regarding the transient behaviour, seems to be slow. There is a delay in the time taken by the thermal emulator to reach the set-point of the MGT. This effect is due to the flow effect, as it is not being controlled to reach the steady state. This will be a future task to optimize the transient behaviour. The second stage refers to the steady state. Here it could be appreciated the effect of the implemented PI controller. As we can see in the result, fluctuation is more or less constant around the set-point so we conclude that it is a valid PI controller.

Chapter 5

Conclusions

Data compilation done through different chapters leads to a bunch of conclusion. Before going into really specific conclusion, the main target has been successfully completed: being able to compare and contrast results of MGT and Thermal emulator with a considerable accuracy. We have demonstrated that indeed the possibility of using a thermal emulator to emulate with high precision the behavior of the MGT is real and possible. It is true, however, that this is a first stage of the project and further research should be done on this topic. The first step is always the most difficult to complete, the path has already begun. The idea now is to follow with this research and try to optimise this thermal emulator in the future not only to be able to emulate this MGT, but with an accurate model, to be able to emulate different thermal devices.

Regarding these first result on the thermal emulator, some decision should be taken. First of all, we believe that changing 2 elements from the set-up is vital. On the one hand, the valve. It is a really slow valve, that causes pressure drop instabilities and that is going to be only used reduce the minimum OP of the pump. A faster one should be implemented, as the presence of a electric valve is a must in this set-up so as to enlarge the flexibility. On the other hand, the mass flow sensor should be changed by a higher range one. It works correctly and really accurately, but having a range up to 25l/min limits the operation of the flow and that is not admissible, as long as we have the power.

At the same time, making an appointment on the thermal power is a must as it is the main target of this research. As we have commented in previous chapters, there are two ways by we could affect this thermal power: flow and electric power. The thing is that according to the results, the main element to increase the thermal power is making use of the electric power. Flow, however, will be used to control the transient state and it will be really important as well in this feature. Therefore, it is important to have an accurate control of both variables not only to control the steady state, but to control the transient as well. At this point, we are able to control the steady state thanks to the PI installed to control the electric power. Installing a PI for the flow was out of this project scope, but it will be really recommendable in further developments of this project. The goal of this PI controller should be controlling the HE output temperature, maintaining it at 55°C and actuating on the flow signal.

This flow control should be done always by the pump signal, instead of the valve signal. Pump plots have shown that the change in flow is fast, with non-delay and symmetric. This is a great advantage as the PI control will be much more stable. Furthermore, we have seen that the pump gives us the opportunity to change the maximal rotation speed value and, therefore, we can obtain a wide range of OP. That is a total win-win.

To finish with, I would say that this is a little piece of what this thermal emulator could achieve. We have seen its potential with simple and non-optimised models, having extremely good results. The objective in the future, therefore, is keep working on this device because its projection is really astonishing in economical, flexibility and operational terms.

Appendix A

Appendix

In this chapter there are going to be shown the Matlab Simscape model full model, electrical sensor input and output connection regarding RTDS cards and the full laboratory sketch used for the set-up. Further Maple calculation are going to be attached with this document to be more efficient.

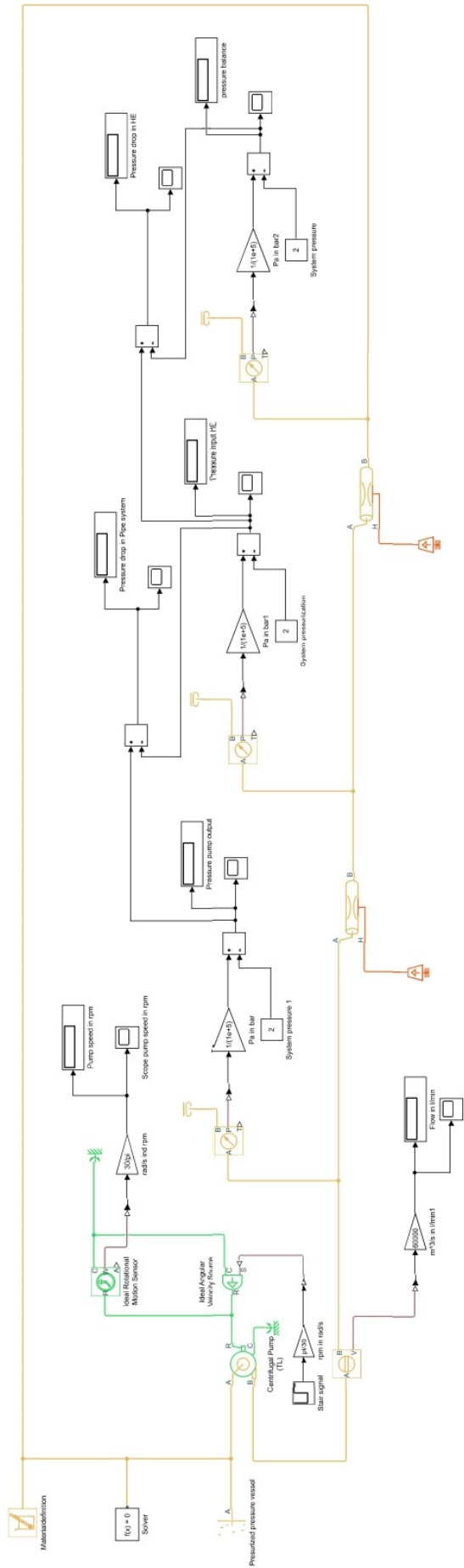


Figure A.1: Matlab Simscape full model

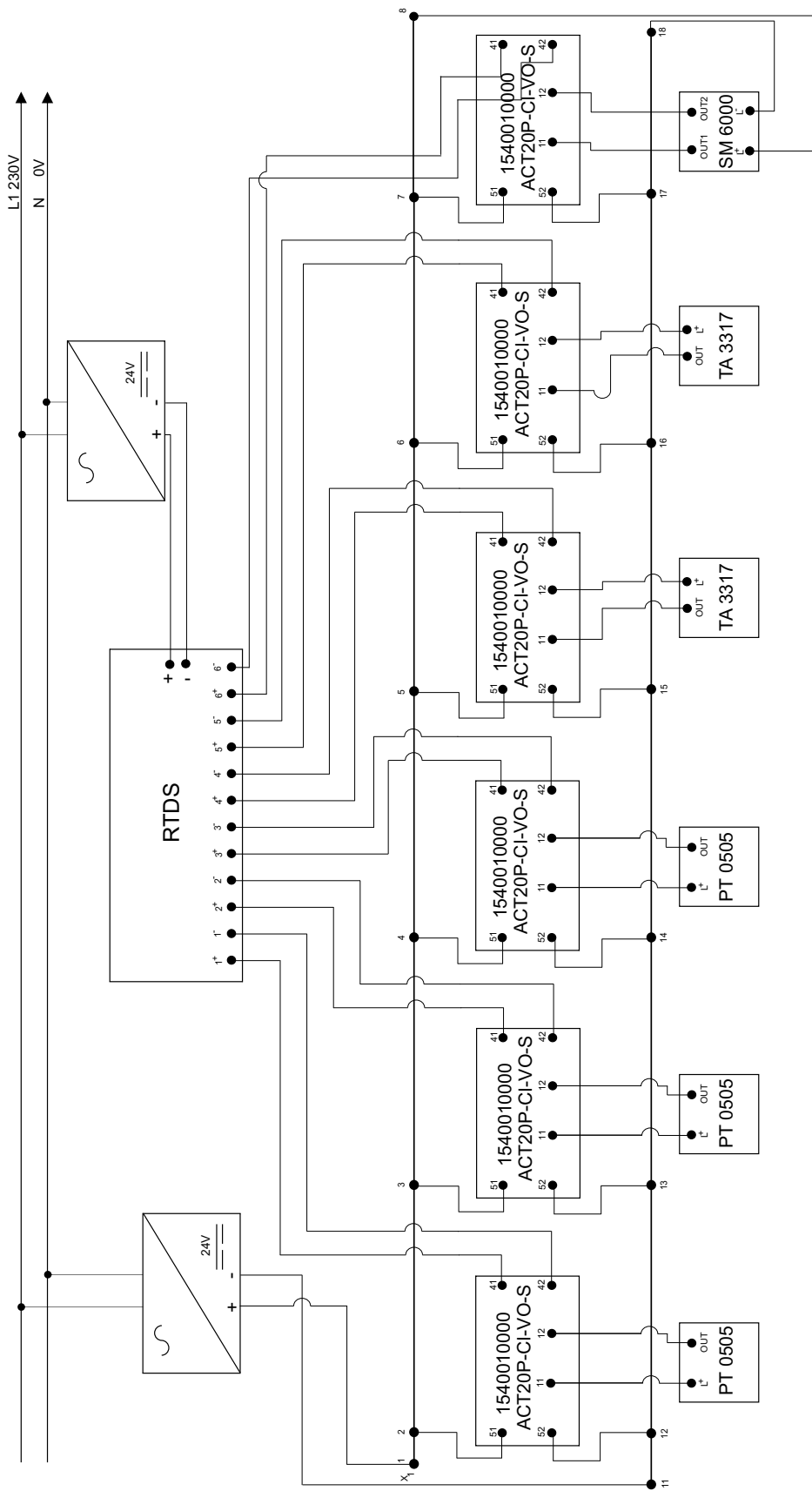


Figure A.2: Sensor electrical connection input GTAI RTDS card

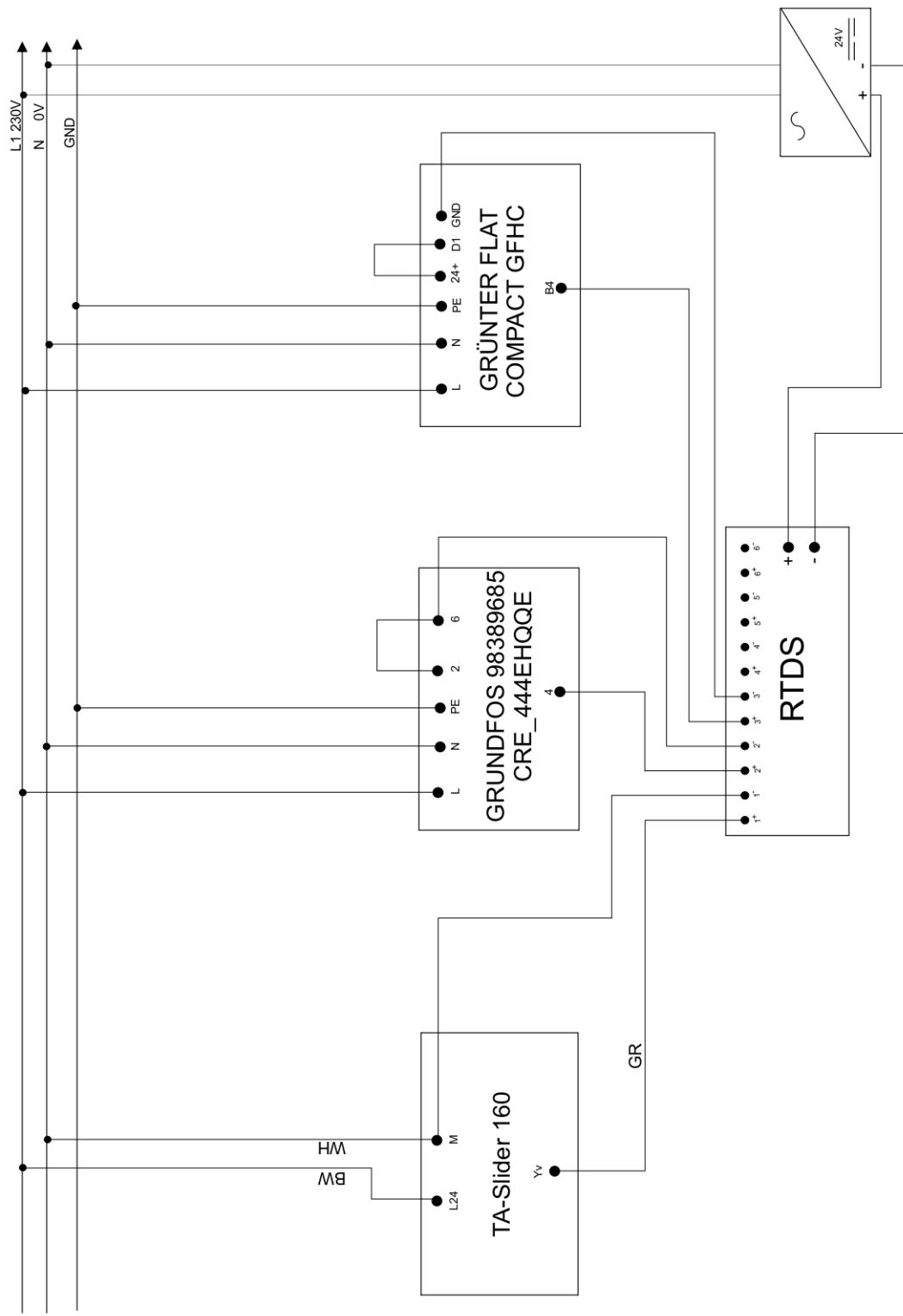


Figure A.3: Principal elements electrical connection output GTA0 RTDS card

Bibliography

- [1] R. Boukhanouf. “Small and Micro Combined Heat and Power (CHP) Systems”. In: *Computer Aided Chemical Engineering* (2011).
- [2] Dejan Brkić. *Review of explicit approximations to the Colebrook relation for flow friction*. 2011. URL: (<https://hal.archives-ouvertes.fr/hal-01586547>).
- [3] Walser Co. *DLE Anleitung - Walser + Co. AG*. URL: (<https://www.yumpu.com/de/document/view/29422945/dle-anleitung-walser-co-ag>).
- [4] Bentley HAMMER CONNECT. *Pressure network hydraulics, Pump Theory*. URL: (<https://docs.bentley.com/LiveContent/web/Bentley20HAMMER20SS6-v1/en/GUID-6BF62F35-5625-48E9-B643-3D41B09B4638.html>).
- [5] Diffen. *Gas vs. Electric Water Heater*. URL: (https://www.diffen.com/difference/Electric_Water_Heater_vs_Gas_Water_Heater).
- [6] Engineers Edge. *Moody Chart*. URL: (https://www.engineersedge.com/fluid_flow/pressure_drop/moody_chart.htm).
- [7] IMI Hydronic Engineering. *TA Slider 160*. URL: (<https://www.imi-hydronic.com/es/product/taslider-160>).
- [8] Michael Smith Engineers. *Useful information on centrifugal pumps*. URL: (<https://www.michael-smith-engineers.co.uk/resources/useful-info/centrifugal-pumps>).
- [9] Günter. *Flat COMPACT Rückkühler*. URL: (<https://www.guentner.de/produkte/rueckkuehler/compact/flat-compact-dc>).
- [10] IFM. *Magnetic-inductive flow meter SM6000*. URL: (<https://www.ifm.com/il/en/product/SM6000>).
- [11] IFM. *Pressure transmitter PT0505*. URL: (<https://www.ifm.com/il/en/product/PT0505>).
- [12] IFM. *Temperature transmitter TA3317*. URL: (<https://www.ifm.com/il/en/product/TA3317>).
- [13] JCGM. *Evaluation of measurement data — Guide to the expression of uncertainty in measurement*. URL: (https://www.bipm.org/documents/20126/2071204/JCGM_100_2008_E.pdf/cb0ef43f-baa5-11cf-3f85-4dcd86f77bd6).
- [14] Grundfos Pump. *Technische Daten CRE 3-4 A-A-A-E-HQQE*. URL: (<https://product-selection.grundfos.com/ch/products/cr-cre-cri-crie-crne-crt-crte/cre/cre-3-4-98389685?tab=variant-curves&pumpsystemid=1568682311>).
- [15] All pumps. *Classification of pumps*. URL: (<https://allpumps.com.au/classification-of-pumps/>).
- [16] Dusan P. Sekulic Ramesh K. Shah. *Chapter 2 - Overview of Heat Exchanger Methodology*. 2003, pp. 78–96.
- [17] Stefan Rauscher. “Modelica Training”. In: *TLK energy* (2022).
- [18] Reflex. *Reflex Reflex N 25, Membran-Druckausdehnungsgefäß, grau, 4/1.5 bar*. URL: (https://www.reflex-winkelmann.com/produkte/reflex_products/8206301/).

- [19] Bill Rehm. *Situational problems in MPD-Reynolds Number*. 2008. URL: (<https://www.sciencedirect.com/science/article/pii/B9781933762241500085>).
- [20] Rena, Pratibha Gautam, and Sunil Kumar. "Landfill Gas as an Energy Source". In: *Current Developments in Biotechnology and Bioengineering* (2019).
- [21] Matt Risinger. *3 Things They Don't Tell You About Tankless*. URL: (<https://www.youtube.com/watch?v=8RFuFBI3r2c>).
- [22] Spitzenberger Spies. *Technische Datenblätter*. URL: (<https://spitzenberger.de/Infomaterial-EMV-Produkte.aspx>).
- [23] Strom-Forschung. *Energy transition in the electricity sector*. 2021. URL: <https://www.strom-forschung.de/research-topics/energy-transition-in-the-electricity-sector>.
- [24] Strom-Forschung. *Thermal power plants: Gas turbines, a building block of the energy transition*. 2019. URL: <https://www.strom-forschung.de/projects/thermal-power-plants/gas-turbines-a-building-block-of-the-energy-transition>.
- [25] Linqip Technews. *How Does a Hydraulic Pump Work? A Definitive Guide*. 2020. URL: <https://www.linqip.com/blog/hydraulic-pump-working-principles/>.
- [26] RTDS Technologies. *Simulation Hardware*. URL: (<https://www.rtds.com/technology/simulation-hardware/>).
- [27] Engineering ToolBox. *Energy Equation - Pressure Loss vs. Head Loss*. 2003. URL: https://www.engineeringtoolbox.com/major-loss-ducts-tubes-d_459.html.
- [28] Land Mark Home Warranty. *How a Water Heater works*. URL: (<https://www.landmarkhw.com/resources/plumbing/how-a-water-heater-works/2/12>).